ELECTRICAL APPAROACHES FOR SELECTIVE DETECTION OF CANCER BIOMARKER PROTEINS WITH APTAMERS

by

PRIYANKA PACHAMPETTAI RAMACHANDRAN

Presented to the Faculty of the Graduate School of

The University of Texas at Arlington in Partial Fulfillment

of the Requirements

for the Degree of

MASTER OF SCIENCE IN BIOMEDICAL ENGINEERING

THE UNIVERSITY OF TEXAS AT ARLINGTON

DECEMBER 2009

ACKNOWLEDGEMENTS

All praises and thanks to the God Almighty for without His blessings and guidance nothing is possible.

I would like to thank Dr. Samir Iqbal for giving me such a wonderful opportunity to work in his laboratory and for being my advisor. Dr. Iqbal has always been a strong sense of support and encouragement at every step of the way. He has taught me to question everything and seek answers, the first trait defining a researcher. His constant motivations have helped cross many a hurdle.

I would also like to thank Dr. Shawn Christensen for giving me access to his lab to perform many of the experiments. His enthusiasm towards research has encouraged me to never give up easily when presented with a daunting problem. I would also like to thank Dr. Young-tae Kim and Dr. Kytai Nguyen for having spared their valuable time to review my work.

I would like to acknowledge my friends Swati Goyal and Kailash Karthikeyan for being with me throughout all the highs and lows of research. The many hours spent in discussions and brainstorming have helped me become more innovative and generate solutions to many problems faced in research. I would also like to thank my friends and co-workers Mohammud Noor, Waseem Asghar and Yuan Wan without whose timely help the projects could not have been completed. I would also like to thank my friends from the lab –Syed Hassan Shah and Ahmed Shahid for their continuous support. I would also like to acknowledge the staff of Nanotechnology Research and Teaching Facility for their patience and assistance with me in the clean room.

I am nothing without my family and I am grateful for their unstinting support and prayers in all of my endeavors.

November 18, 2009

ABSTRACT

ELECTRICAL APPAROACHES FOR SELECTIVE DETECTION OF CANCER BIOMARKER PROTEINS WITH APTAMERS

Priyanka Ramachandran, M.S.

The University of Texas at Arlington, 2008

Supervising Professor: Dr. Samir Iqbal

Cancer is a disease that is the central focus of many a researcher's attention. As it is a disease that can spread very rapidly and can be fatal in many cases, its early detection and early treatment can dramatically change mortality. Towards the early detection of the disease, antibodies are most commonly used for the detection of cancer biomarkers. The use of antibodies in diagnostics has proven fruitful in the past. But advancements in molecular biology have introduced aptamers for diagnostic and therapeutic purposes. Aptamers are oligonucleotides or peptides that are usually synthesized by a selective process called SELEX. Aptamers are more advantageous as they are stable over wider physical conditions and have higher selectivity than antibodies.

The Epidermal Growth Factor Receptor (EGFR) is a cell surface protein that plays a pivotal role during the tumorigenesis of the cancer cells. It is over-expressed during the onset and the course of

cancer. A biomarker sensor was designed to electrically detect proteins. For initial studies, the capture of R2Bm protein was demonstrated using double-stranded DNA that binds to it. Towards a practical application of the detection approach, EGFR capture and detection was also done. The EGFR was captured by the anti-EGFR RNA aptamer. To electrically detect the presence of the proteins, a Complementary Metal Oxide Semiconductor chip was fabricated with gold nano-electrodes for sensitive electrical detection of two model proteins. The electrical data obtained showed an increase in current by three orders when protein was captured between nano-electrodes in comparison with the control chips. The presence of the protein and the selective agent was optically confirmed in both cases. The use of CMOS chips in the detection system makes integration with other circuits units more feasible. Designing a microarray for the simultaneous electrical detection of many biomarkers is also possible. Also, to test the prototype device and technology of guided-more resonance, the EGFR aptamer was immobilized on a titanium dioxide surface. The technology involves the analysis of shift in wavelength after a binding event. Upon analysis it was found that the protein was indeed bound to the aptamer on the titanium dioxide surface.

TABLE OF CONTENTS

LIST OF ILLUSTRATIONS

Figure Page

LIST OF TABLES

Table Page

CHAPTER 1

INTRODUCTION

Cancer is a deadly disease that leads to death if not detected and treated at the right time. The diagnosis of cancer is a very important aspect of cancer treatment. The earlier diagnosis always proves to be better. There are numerous methods of cancer detection available in the market today that aid in detection. To design a device that can detect the presence of cancer biomarkers in the presence of a large background noise would be the ideal scenario. Antibodies are commonly used to functionalize nano-devices and nano-objects for detection of specific biomarkers. Such antibody-based molecular recognition has limited capability for field-deployable or point-of-care modalities, as antibodies need certain range of temperatures, humidity and solution conditions to retain their structure. In terms of the solution conditions, an important parameter is the need for low ionic strength. Low ionic strength of the buffer solutions is needed to overcome surface Debye screening, but it also results in weaker interactions between the surface probe and solution target molecules. A possible solution is the development of non antibody-based interactions that are at least as selective as antibody-based assays.

The thesis explores the design of biochips that can enable early detection with the aid of aptamers. Chapter 2 gives a brief background on the technologies and biological molecules used. Chapter 3 discusses the fabrication of a break junction chip. Chapter 4 discusses the design and development of a silicon oxide CMOS chip that was designed and tested with double stranded DNA and its binding protein – R2Bm. The measurements of electrical detection of the dsDNA and the protein bound to the DNA are presented. In chapter 5, the electrical detection of EGFR, a cancer biomarker

protein, on a similar silicon oxide CMOS chip utilizing complementary binding from EGFR RNA aptamer, is discussed. Chapter 6 discusses the detection of the cancer biomarker protein EGFR by EGFR RNA aptamer on titanium dioxide. The alternate attachment surface is to allow for more methods of cancer protein detection using RNA aptamer.

1.1 Electrical detection of R2Bm protein using silicon chip

R2Bm is a retrotransposon protein found in the organism *Bombyx mori*. In chapter 3, the immobilization of double stranded DNA (dsDNA) on the silicon oxide surface is discussed. The chapter also discusses the binding of the R2Bm protein with the dsDNA. The binding between the dsDNA and the protein molecule was confirmed optically using a fluorescent dye. Electrical measurements performed on the CMOS chip confirmed the presence of the dsDNA and the protein on the chip surface.

1.2 Break Junction Fabrication using FIB

Break junction is an electrical junction formed from thin metal strips. Chapter 4 discusses the fabrication of these break junctions on CMOS chips. Focused Ion Beam (FIB) was used to scratch thin metal lines and subsequent electromigration was done to create break junctions in a controlled manner.

1.3 Electrical detection of EGFR protein by EGFR aptamer using silicon chip

EGFR is a receptor protein found on the surface of cancerous cells. The early detection of the receptor can facilitate better and more effective treatment. Chapter 5 discusses the design of the CMOS chip for the protein detection. Aptamers were immobilized on the chip and the protein flown through it was captured. The presence of the protein and the aptamer was initially confirmed by using fluorescent dyes that bind to the aptamer and protein respectively. Electrical measurements that were performed on the chips conclusively proved the presence of the RNA aptamer and the captured protein on the CMOS chip surface.

1.4 Detection of EGFR protein by EGFR aptamer on titanium oxide

In this chapter we discuss the attachment of the aptamer on the surface of the titanium oxide coated silicon chip and the detection of the EGFR protein. The same procedure was adapted to immobilize the RNA aptamer on the surface of titanium oxide titer well plates. The use of titanium oxide plates was to facilitate the detection of protein and aptamer through a different modality of resonant sensing.

.

CHAPTER 2

LITERATURE REVIEW

2.1 Biomarkers

Biomarkers are biological indicators found within the body that give information on the homeostasis of the system. They also help understand when the homeostasis is thrown off balance [1]. These biomarkers can be any biomolecule found within the body. Typically these are hormones, enzymes, cells, molecules, genes or gene products. The name “biomarkers” is used in short for ‘molecular biomarker’ [2]. There are certain levels in which these entities are present under normal conditions. But when a disease condition arises, one or a few of the biomarker levels change. Measuring the levels of the molecules often gives a clearer picture of the organ system under distress.

Proteins have an important role to play in the diagnosis of diseases as their expression is altered during the course of a disease. Technological advances have led to the development of proteomics, which is the study of the structure and function of human proteins in greater detail. The study of these proteins has proven to be the biggest advantage to researchers in the early diagnosis of diseases and also in drug discovery. Advances in proteomics combined with rapid developments in bioinformatics have led to numerous software tools being developed to predict the best selective agents or drugs in numerous diseases. Some of the proteins that aid as disease biomarkers include the amyloid protein that is deposited in the brain in the case of Alzheimer’s disease, or the detection of the thyroid hormones T3 and T4 in cases of Grave’s disease or the presence of specific antibodies in the cases of autoimmune disorders. In the diagnosis of AIDS, the antibodies that are produced against the virus are detected [3-5].

Cells are also very important biomarkers. Cells from virus, protozoa, bacteria and fungi act as biomarkers in numerous infections. In the case of malaria, the organism from the protozoa family *Plasmodium sp.* is detected. In the detection of tuberculosis, the causative organism, *Mycobacterium tuberculosis*, is detected by culturing the bacteria on a petri-dish. Sickle cell anemia which is a genetic disorder affecting the red blood cells, is detected by visualization of the cell shapes.

In the case of cancers, the early detection of the cancer biomarkers is pivotal in effective treatment and recovery. The types of cancer biomarkers can vary depending on the cancer in question, although there are a few common features to all cancers. In the following table, some of the cancers and their biomarkers are mentioned. From the table, it can be seen that the protein EGFR is expressed in most of the mentioned cancers.

Table 2.1. Some cancers and their biomarkers

Disease	**Biomarker**	**References**
Breast Cancer	CEA ,HER-2, EGFR	[6], [7]
Cervical Cancer	Human Pappiloma Virus, EGFR	[8, 9]
Hepatocellular Carcinoma	alpha – fetoprotein	[10]
Lung Cancer	EGFR , KRAS, BRAF	[11, 12]
Bladder Cancer	EGFR , fatty acid binding protein, HSP 27, Annexin	[13, 14]
Ovarian Cancer	EGFR, haptaglobin α, CA-125	[15-17]
Esophageal Cancer	EGFR, periplakin	[18, 19]

The discovery and validation of new biomarkers in conjunction with the technological advances paves way for the design of better and more sensitive diagnostic methods.

2.2 Detection of Proteins

Protein detection has taken center stage with ever more understanding of disease pathways and cell signals. There are currently numerous methods available for the detection of proteins. The methods of protein detection can be broadly classified as labeled detection and label-free detection. Labeled detection methods utilize a secondary organic, inorganic or radioactive molecule to bind to the protein in order to visualize or confirm the presence of the protein. For example, fluorescent dyes such as Alexa 350, 488, etc, bind to antibodies that are specific to the proteins of interest. They are then detected with a fluorescent microscope. Some proteins are tagged with radioactive agents and the radioactivity is measured.

In order to detect a protein, selective agents are commonly used. Selective agents are those that specifically capture the protein of interest. They could be antibodies, chemical molecules, nucleic acids, etc. Traditionally, the detection of proteins is done by developing monoclonal antibodies or isolating the antibodies against the protein of interest. They are then allowed to bind and the antibodies are stained. This basic process has developed and given way to different protein detection assays detected mostly by antibodies in analytical formats like Enzyme Linked Immuno Sorbent Assay (ELISA), immunobead assay, western blotting, microarrays, etc. As the thesis is about the development of a biosensor for the detection of cancer, they will be dealt with in more detail than the other methods.

Biosensors are commonly defined as transducers that provide quantitative or semi – quantitative analysis. A biosensor consists of a biological molecule that recognizes the target molecule and a transducer element that utilizes the principles of mass, optical, thermal or electrochemical changes.

Optical biosensors utilize the properties of light waves such as diffraction and reflection in the biosensor design. The most reported methods of optical detection are Surface Plasmon Resonance (SPR), fluorescence anisotropy and luminescence detection [20].

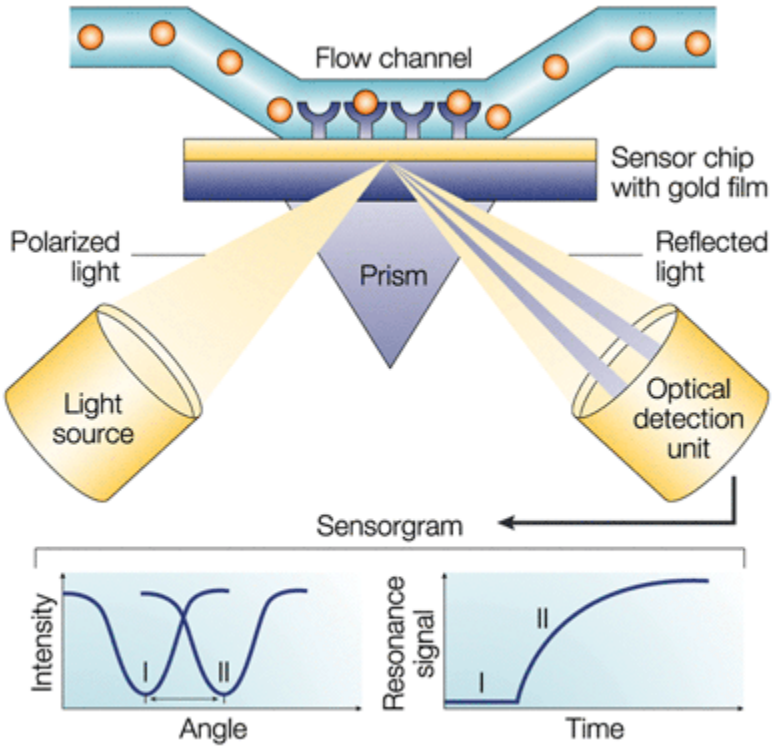

Figure 2.1. Representation of an SPR setup. Reprinted by permission from Macmillan Publishers Ltd: [Nature Reviews Drug Discovery] [21], copyright (2002)

Mass sensitive biosensors have also been reported. Some of these use the microgravimetric methods of analysis performed on piezo-electric quartz crystals. They measure change in the resonant frequency of the signal is measured as a direct function of the change in the mass [20].

Potentiometric biosensors are those that measure the potential difference between two electrodes – a working and a reference electrode. Field-effect transistors (FETs) are the most commonly used types of devices in this class. Complementary metal-oxide semiconductor (CMOS) devices and Carbon nanotube FETs are the latest in potentiometric biosensors as they allow for miniaturization of the device as well. The devices discussed in chapter 3 and 4 belong to this class as well [20].

Electrochemical based biosensors are going to be discussed further in this section. There have been biosensors reported that use electrochemical transduction. Some of the methods include differential pulse voltammetry, alternating current voltammetry, square wave voltammetry, potentiometry or amperometry. The common factor between all these methods is that the outcome can be read as an increase or decrease in the output signal. Electrochemical impedance spectroscopy has been used to detect IgE molecules in a label-free manner [22]. Real – time monitoring of the sensor signal has been possible with impedance sensors. Impedance sensors allow the real-time monitoring of the signal and provide new insights into ligand-analyte interaction kinetics. With impedance measurements, a negative readout signal is obtained due to an increase in electron transfer resistance. However, there have been reports describing a positive readout signal due to the change of the surface charge from positive to negative when the protein is captured at the appropriate pH level [23].

Electrical measurements allow for protein detection without the use of dyes. In some cases, metals, metal oxides or semiconductor nanoparticles such as Ag_2S, CdS, CdSe, and TiO_2 are used as nanoparticle tags in electrical assays with increased sensitivity [24].

With advances in nanotechnology, nanowires are also being used to design novel devices. Nanowire arrays have been reported for the detection of proteins. They employ nanoscale wires made from metals and semiconducting materials such as silicon [25, 26]. Microcantilevers have also been developed for the detection of biological molecules and proteins in particular. Microcantilevers can operate in two modes – cantilever bending and resonance response variation [27]. Carbon nanotubes are also being used for the detection of the proteins. Single-wall carbon nanaotubes (SWNT) are grown and the appropriate surface chemistry is performed on these to attach the selective agent and bind the protein of interest [28-30].

The Table 2.2 gives a comparison of the advanced methods of protein detection, the selective agents employed, and sensitivities that have been achieved for the protein detection.

Table 2.2. Different protein detection methods, signal amplification and detection sensitivity

Method	Signal amplification	Detection sensitivity	References
SPR	None	130 ng/mL of Folate Binding Protein (FBP)	[31]
QCM	Au nanoparticles	1.5 ng/mL FBP	[32]
ELISA	Enzyme	5-100 ng/mL	[33]
Optical Diffraction	Enzyme	50 pg/mL	[34]

2.3 Aptamers

The recent developments in the field of molecular biology and genetics have led to development of novel affinity binding agents such as aptamers. Aptamers are short lengths of peptide or nucleic acids synthesized with specific binding affinity for proteins, drugs and any other small molecule. Aptamers have been synthesized against a variety of molecules. A few sample aptamers that have been used for molecular scale sensing include: (a) RT-26: a high-affinity DNA aptamer than can be used for the detection of the reverse transcriptase of the HIV type-1 as the target protein [35, 36]; (b) Anti-thrombin aptamer identified to interact with thrombin protein [37]; (c) 45-mer long aptamer for rapid detection of immunoglobulin E. High level of IgE is seen in patients with allergic asthma & immune deficiency-related diseases, such as AIDS [38]; (d) RNA aptamers for the detection of β-amyloid peptide [39]. The Alzheimer's disease is characterized by the deposition of this peptide in the brain. (e) A host of DNA/ RNA aptamers for bio-warfare agents' detection like ricin [40, 41].

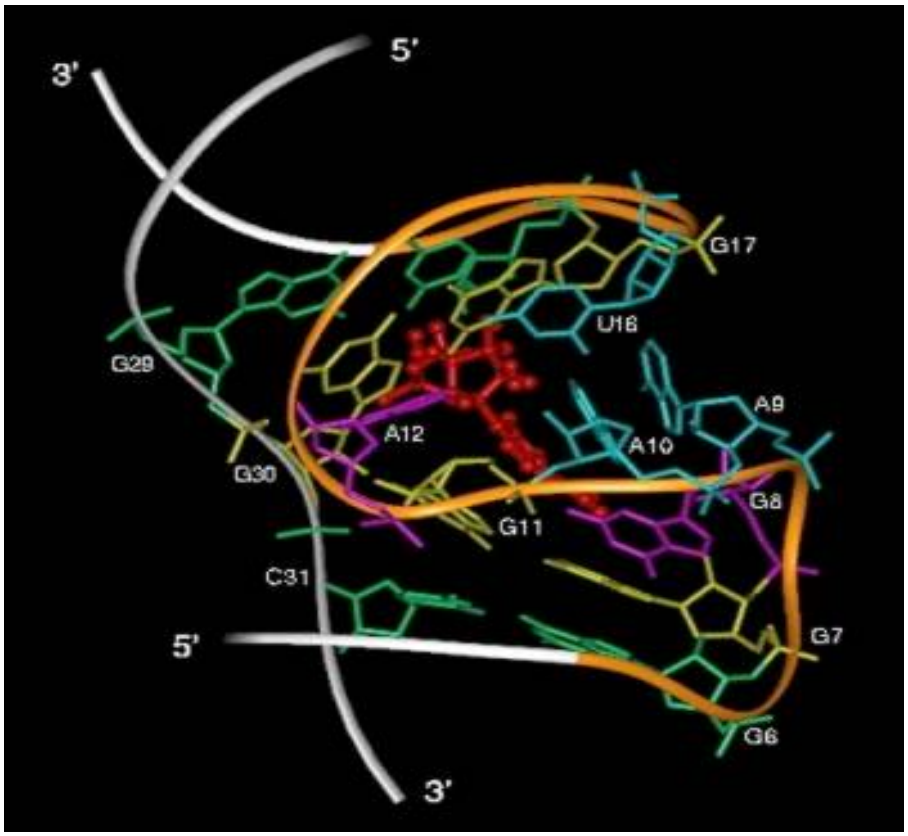

Figure 2.2. ATP binding RNA aptamer. Reprinted from [42] Copyright (2007), with permission from Elsevier

Aptamers exhibit high binding affinities with dissociation constants in the sub nano molar range for even closely related isoforms of proteins [43, 44]. The distinctive binding abilities of aptamer arise from its recognition of protein folding that play an important role in the functioning of the protein. It has also been observed by us and other researchers that aptamers retain their binding and recognition ability even upon immobilization on a surface. This flexibility allows for the application of aptamers in areas of purification, drug targeting, diagnosis and therapy [45-47].

DNA or RNA aptamers can be routinely isolated from synthetic combinatorial nucleic acid libraries by an *in vitro* automated process called SELEX (Systematic Evolution of Ligands by Exponential Enrichment) [48]. Random pools of nucleic acids are screened for ability to bind to a selected molecule. Through repeated cycles of the process, aptamers selective to the small molecule of interest are isolated

[49]. Several sequential steps are common to all aptamer *in vitro* selections. Iterative rounds of selection and amplification are performed until the target-interacting sequences dominate the population. Over the last few years, considerable efforts have focused on automating in vitro selection procedures [50, 51]. Typically 6 to 18 iterative cycles of selection and amplification are required to generate suitable aptamers from a starting library. Within only a few weeks, aptamers for multiple targets can be selected and characterized in parallel, making aptamers rapidly available for the life sciences industry.

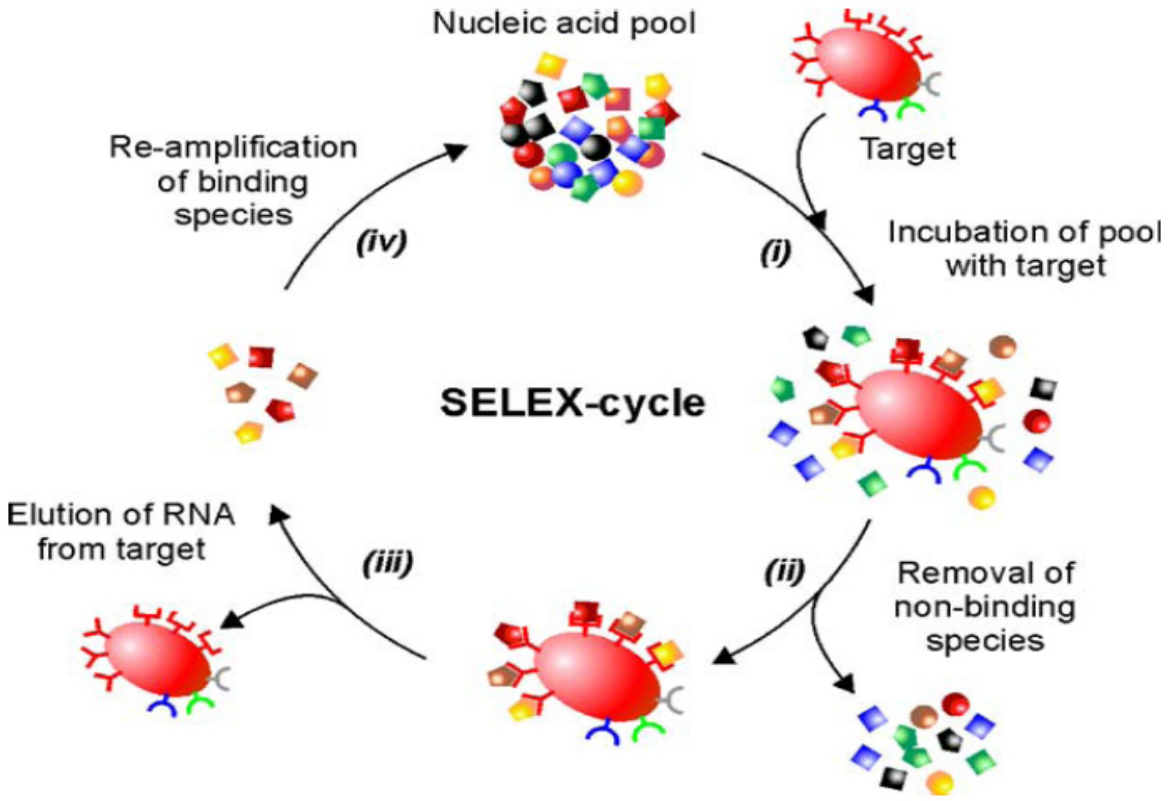

Figure 2.3. Diagrammatic representation of the SELEX process [52]. With kind permission from Springer Science+Business Media: Applied Microbiology and Biotechnology, Aptamers—basic research, drug development, and clinical applications, 69, 2005, Daniela Proske

2.4 Antibodies and Aptamers

Aptamers and antibodies have similar functions in that they recognize and bind to specific molecules. Aptamers have certain advantages over antibodies. Aptamers are synthesized *in vitro* while antibodies require an *in vivo* approach. The usage of animals necessitates the induction of an immune system and the sensitivity of distinction between closely related proteins (toxins) maybe lost. Such is not the case with aptamers. As antibodies are obtained from a biological source, they need to be handled in close to physiological conditions. Aptamers, on the other hand are stable at higher temperatures and they can be regenerated easily upon denaturation. Aptamers have longer shelf life than antibodies. In most cases, further modifications of the antibody are not possible as that would interfere with the paratopic region. There are disadvantages associated with aptamers as well. They can be expensive to manufacture on a larger scale.

2.5 DNA Immobilization on Surfaces

Through the years there have been many reports on nucleic acid attachment and detection on many different types of surfaces. A large number of these attachments are done by modifying the DNA molecule. Most common modifications are thiol, amino with various spacer lengths, biotin, diaminopurine, 2'-aminopurine, 5'-bromo, 5'-methyl, 5'-nitroindole and various fluorescent markers. These modifications are made to either the 3' or 5' ends of the molecule. These modifications made to the DNA molecule can confer changes to its properties. Changes can be seen in its molecular weight and melting temperature to name some. The modifications are done to the DNA molecules in order to aid in better immobilization on surfaces. Self-assembled monolayers (SAMs) are formed from variety of molecules, which stem from underlying forces that have affinities for a specific surface or chemical groups. SAMs are a simple and convenient method to modify the surface properties of metals, metal oxides and semiconductors. They are produced as organic assemblies by the adsorption of organic constituents from the solution or liquid phase. The organization of the organic constituents is specific based on affinities which the molecules

have for the surfaces. Molecules forming a SAM usually have a chemical group that has the affinity and is named the ‘headgroup’. SAMs are usually only a few nanometers thick.

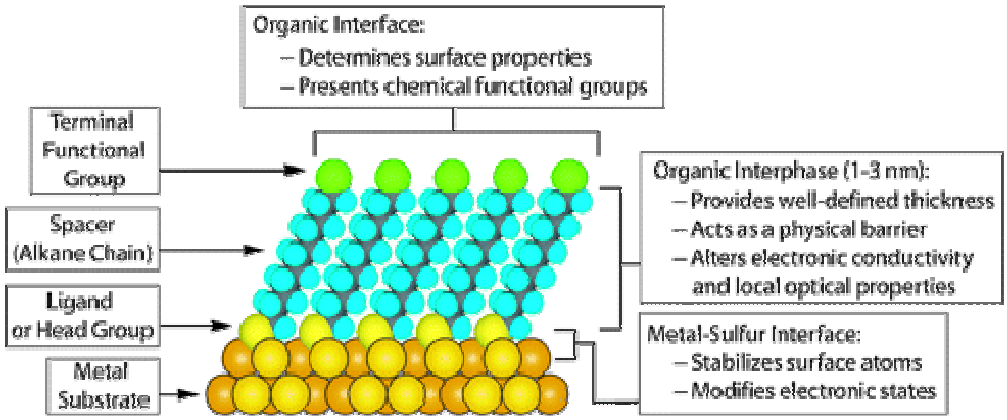

Figure 2.4. Schematic representation of a single-crystalline SAM of alkanethiolates supported on a gold surface with a (111) texture. Reprinted in part with permission from [53]. Copyright 2005 American Chemical Society.

To produce DNA SAMs, the molecules are modified as required. One of the common methods for DNA immobilization is the modification of the DNA with a thiol (-SH) group at the 5’ or 3’ end and allow for self assembly on gold layers or gold nanoparticles. Another common method is to use linker molecules such as 1-ethyl-3-(3-dimethylaminopropyl) carbodiimide (EDC) to bind to surfaces that have a carboxy (-COOH) group on them. EDC is often used in combination with N-hydroxysuccinimide (NHS) in order to increase stability and make an amine-reactive product. The presence of the amine group makes it possible to make more attachment chemistries. Another common method of DNA immobilization is the introduction of biotin modification on the 5’ or 3’ end to allow binding with a surface modified with streptavidin or vice versa.

Just as the DNA molecule goes through some modifications for better immobilizations, so does the surface. One of the most widely done modifications is the introduction of the silane layer on the surface. This is done by the application of many chemicals which possess the silane group. Silicon oxide

surfaces can be modified with a silane layer or an epoxide layer. After modification, the surface properties completely change, usually making it more suitable for DNA immobilization. Generally, in order to make the DNA immobilizations stable for other processes, Magnesium ions are also included in the DNA buffers. These ions serve to shield the negative charge of the DNA molecule. Some of the common surface and the best suited DNA modifications are listed below in Table 2.3.

Table 2.3. Common methods to immobilize DNA on surfaces [54]. Sensors and Actuators B: Chemical, 92, P. E. Lobert, D. Bourgeois, R. Pampin, A. Akheyar, L. M. Hagelsieb, D. Flandre and J. Remacle, Reprinted from Immobilization of DNA on CMOS compatible materials , 8, Copyright (2003), with permission from Elsevier

Protocols	Support activation[a]	DNA modification[a]	Link between DNA and the modified support
(a)	Polylysine coated support: 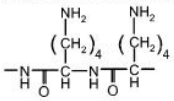	Non-modified DNA	
(b)	1-Vinyl silanized support: 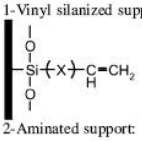 2-Aminated support: 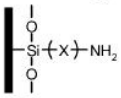 3-Polystyrene or polymethyl-metacrylate (PMMA) coated support	Non-modified DNA	Non-covalent hydrophobic interaction
(c)	Thiol-modified support: 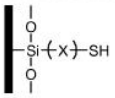	Disulfide-modified DNA: R1-S-S-R-oligomer	Disulfide bond: 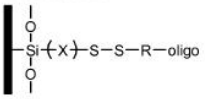
(d)	Aldehyded support: 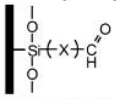	Aminated DNA: NH_2-oligomer	Imine bond: 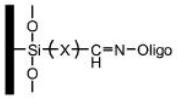
	Epoxide activated support: 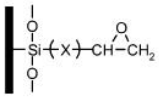	Aminated DNA: NH_2-oligomer	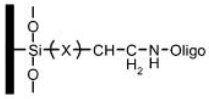
(e)	Aminated support: 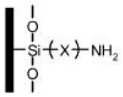	Thiolated DNA: HS-oligomer + Cross-linker with a maleimide and a succinimide ester moiety	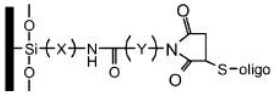
Aldehyded process	Aldehyded support: 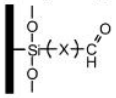	Aminated DNA: NH_2-oligomer	Imine bond: 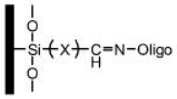
Aminated process	Aminated support: 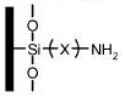	Aldehyded DNA: HOC-oligomer	Imine bond: 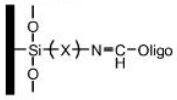

2.6 EGFR Protein

Epidermal Growth Factor Receptor (EGFR) is a protein located on the cell surfaces – normal and cancerous [55]. It belongs to the ErbB family of receptors. It is the receptor that binds growth factors and upon activation induces proliferation and differentiation. The receptor upon binding with a growth factor activates tyrosine kinase, an enzyme found inside the cell. One of the major activation factors of the cascade is the dimerization of the receptor from its monomer stage. The tyrosine kinase in turn activates a cascade of reactions resulting in the activation of DNA synthesis, cell growth and also the activation of oncogenes *fos* and *jun* [56]. The protein is made of 1186 amino acids. and is used as a drug target for the treatment of some cancers. EGFR has also been used as a cancer marker for the disease progression in a number of cases such as breast cancer [7], ovarian cancer [16], bladder cancer [13] and esophageal cancer [18] among others.

2.7 R2Bm DNA and Protein

R2 is a part of the DNA that codes for a single polypeptide sequence that has a reverse transcriptase, nucleic acid endonuclease and nucleic – acid binding domains. It is also a non long terminal repeat (non LTR) retrotransposon [57]. It is specifically found in the 28S rRNA genes in many eukaryotes [58, 59]. Retrotransposons are DNA elements found in eukaryotes that are reverse transcribed to RNA and then to DNA again. During the process of retrotransposition, mutations that are formed remain stable and are included in the genome. Retrotransposons are mainly of two types, those with a long terminal repeat (LTR) and those without a long terminal repeat sequence (non LTR). The R2 element has a central reverse transcriptase domain, a C – terminal domain and an N – terminal domain with a C_2H_2 Zinc Finger and a Myb – like nucleic acid binding motif [58, 60]. The R2Bm protein binds the dsDNA of the organism *Bombyx mori* in the Myb domain [57]. The zinc finger and Myb motifs of the protein bind to the dsDNA sequence described in [57, 61].

Bombyx mori is the domesticated silk moth, the caterpillar of which is commonly known as silkworm. Silk is obtained from the cocoon of these caterpillars. It is of immense economic importance in many countries. As these organisms are large in size and also easy to culture, they are widely used in biology research. The genome of the insect has been studied extensively. Many advances in biology have been enabled by studies performed on the silk moth.

2.8 CMOS Technology

Integrated circuits make use of the technology of Complementary Metal Oxide Semiconductor (CMOS). CMOS chips are widely used in electronic devices that find applications in research setting and also in everyday usage. They are usually combined with microfluidics devices in the detection of biological molecules [62]. CMOS technology has provided new tools and techniques to fabricate nano-scale devices. CMOS chips can be made with many materials and the many smart-surface approaches that are possible provide capabilities to covalently attach a number of biomolecules on these materials. CMOS can play another crucial role of providing same-chip data-processing and read-out interface [63].

2.9 Break Junctions

The technique of 'Break Junction" was researched in depth by Moreland and co-workers at the National Bureau of Standards [64]. Break junctions are usually the simplest way to study the current flow through molecules. It consists of a thin metal strip in which a gap is formed by one of the many possible ways. The gap that is formed is usually in the nano or sub-nanometer range. The break in the metal strip can be caused by a variety of methods. The most common method uses electromigration.

Electromigration is a break-down phenomenon where application of voltage and current that flows results into a "break" in the metal line. The application of an electric field produces a large current density in the metal strips. When an electric field is applied on the metal strip, the electrons in the metal move under the influence of the large current density. If a charged defect in the metal is encountered, the momentum transfers from the conduction electrons to that defect. In due course of time, the momentum

exchange becomes larger leading to the build-up of a force causing the atoms to move away from the defect. This results in the breakdown of the metal at that point. Added to this, the heating of the wire speeds up the process of breaking. Both the heating and the momentum exchange increase with an increase in the current density in relation with the applied electric field or the applied voltage. Usually, in these experiments, a threshold current is observed. This indicates the existence of an energy threshold required to induce the electromigration of metal atoms. With break junctions, these phenomena are used to break the wires in a controllable and self-limiting manner. These electrodes are then adapted for use in transport studies, and molecular and nanocrystal studies among others.

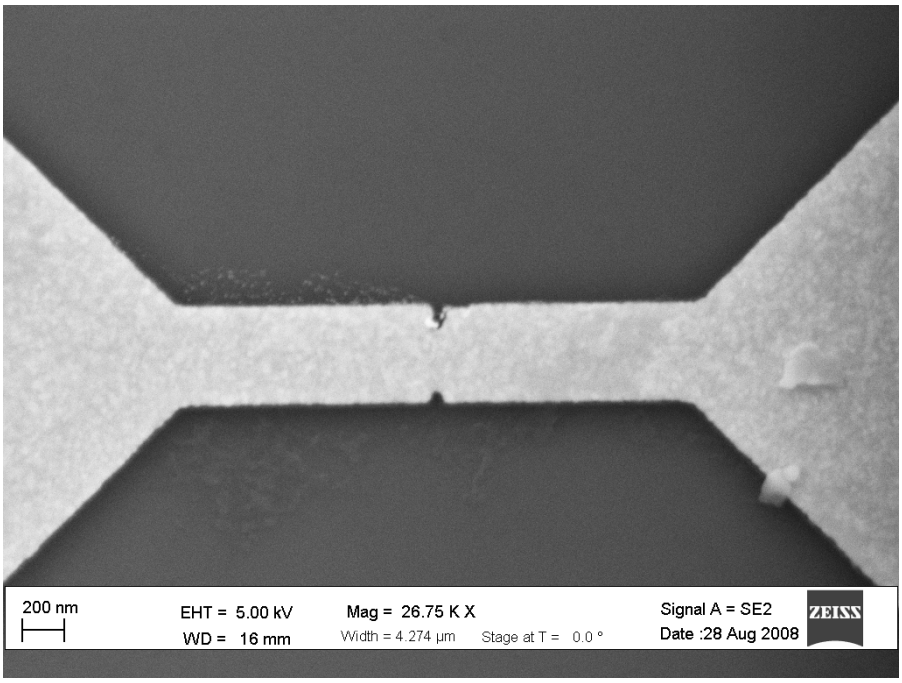

Figure 2.5. SEM Micrograph of a metal line later used to create break junction on a CMOS chip. The chip was fabricated by the processes of E-beam and photolithography.

2.10 Resonant Sensors

The titanium oxide plates described in Chapter 6 are in fact grating structures that are coupled to guided-mode resonance sensors. The sensors are based on the sharp reflected and transmitted spectra produced by the sub wavelength periodic waveguides. When the refractive index or thicknesses of the resonant waveguide grating are changed, there is a change in the resonance frequency noted. A One-dimensional resonant waveguide grating structure have separate reflectance peaks for different polarizations of incident waves. The guided-mode resonance occurs when an incident wave is phase matched to a leaky waveguide mode supported by the waveguide grating structure. For every measurement, two different peaks are available because of the different polarizations. This can be utilized to resolve both thickness and refractive index changes in a single temporal and spatial measurement. This aspect facilitates time resolved protein binding studies to be performed with greater accuracy. The technology also gives efficient reflection peaks with narrow line widths which give very high signal to noise ratio. This translates to reduced power requirements and increased accuracy. This sensor technology can be extended to medical diagnostics, drug development, industrial process control, genomics, environmental monitoring, and homeland security [65-67]. Some of the most marked advantages of the technology are:

- The strong resonant peak response permits the use of low cost light sources and detectors.
- The process allows for label-free sensing enabling real-time detection with no pre- or post-chemical processing.
- High resolution and high signal integrity is obtained because of the well-defined resonance peaks.
- It is possible to differentiate between background changes and target binding events from the multiple data points obtained from multiple resonances.
- Ultra-compact and highly integrated sensor systems can be made.
- The size of the sensor element can be made very small to accommodate high density biochips.

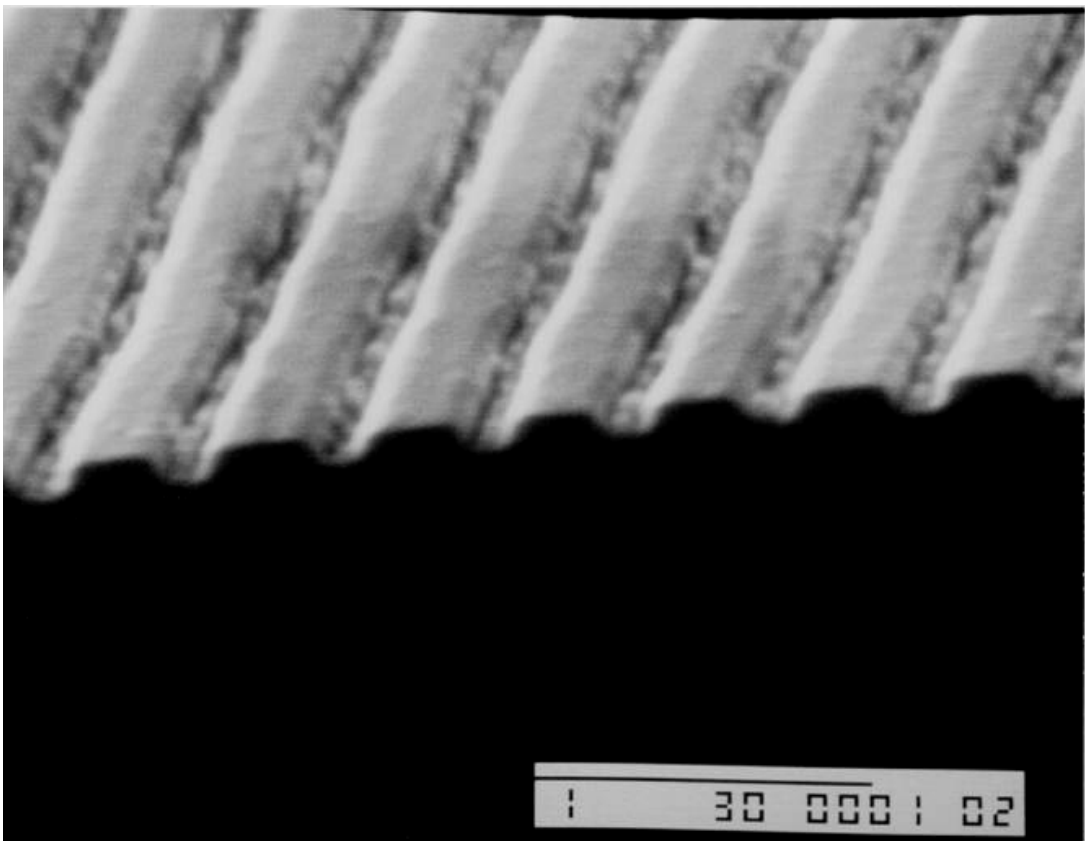

Figure 2.6. Scanning electron micrograph of a fabricated grating based sensor [65]. Obtained from personal communication.

CHAPTER 3

BREAK JUNCTION FABRICATION

3.1 Introduction

Break junctions are electrical junctions between two electrical wires. The wire material is pulled apart electrically or mechanically to produce a gap in the nanoscale range forming electrodes of the electrical wires. This chapter discusses the fabrication of the CMOS chip and the introduction of the break junctions in brief.

3.2 Fabrication of CMOS Chip

The fabrication of the CMOS chip involved a series of processes. Firstly, a specific pattern was chosen for the CMOS chip and a mask was designed using AutoCAD. A 4 inch silicon wafer was used for the fabrication process. The silicon wafer was first oxidized to produce a silicon oxide layer. The first process to be performed was that of photolithography to transfer the pattern on the mask to the silicon wafer.

The break junctions were fabricated through a multi-step process. The processes involved in the fabrication of the break junction are as follows:

1. Preparation of the appropriate mask pattern
2. Photolithography to transfer the pattern on the silicon dioxide wafer
3. E-beam evaporation to deposit the metalized layers(Ti/Au)

4. Lift-off to remove the metal from undesired areas

These steps were performed in order to fabricate the first layer of the gold electrodes. The same processes were repeated in order to obtain the second layer of the probing pads. The chips were fabricated with no gap between the electrodes. After fabrication, the current-voltage characteristics across the electrodes were measured using the *Agilent I-V Probe Station.* Two probes were placed, one on each side of the metal strip and the other on the probing pads to measure the current across the electrodes upon application of a voltage sweep. Then, an FIB process was performed on the chip to make a scratch on the surface of the metal. The FIB process allows for both manual and automated performance. The gold electrodes were scratched by use of a manual process.

The break in the electrodes was finally made by application of a high voltage across the electrodes. This resulted in the formation of nano-gaps at precise locations on metal strips. The *I-V* measurements were recorded before and after the break of the junctions.

3.3 Results

The break junction chip was effectively fabricated by the process mentioned in the previous section. An SEM image of a metal strip from the fabricated chip is presented in Fig. 3.1. After the chip was fabricated FIB scratching was done on the chip (Fig. 3.2). Fig. 3.3 shows the FIB scratch on the surface of the gold electrode. After the FIB scratch was made on the electrodes, a voltage sweep of 0 V to around 7 V was applied on the electrodes in order to break the junction (Fig. 3.3). The electrical data recorded before, during and after the application of the voltage is shown in Figs. 3.4 to 3.6.

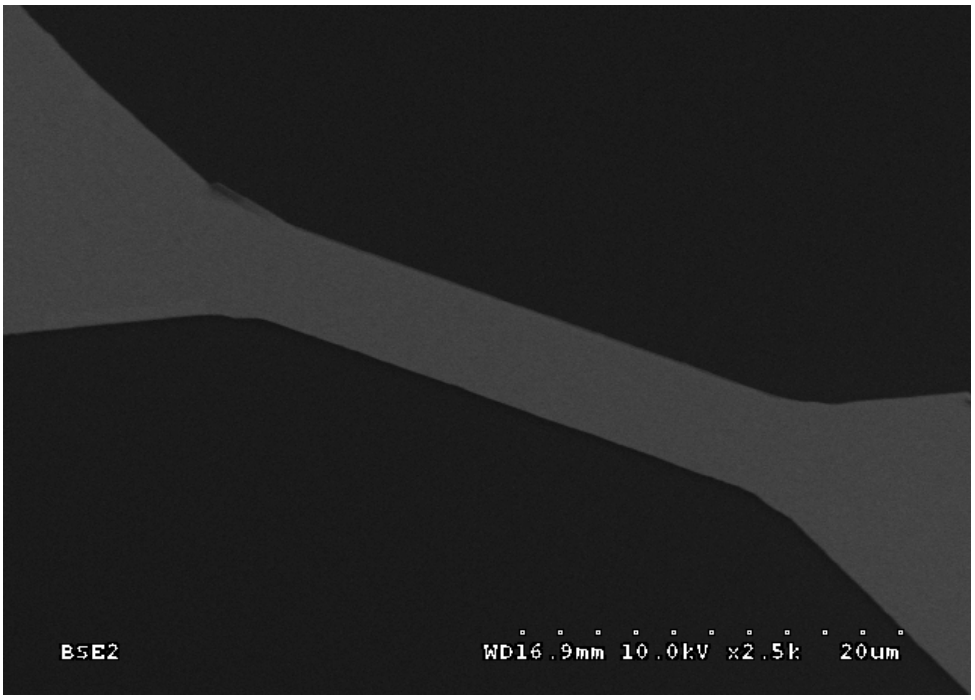

Figure 3.1 SEM micrograph of break-junction chip after fabrication

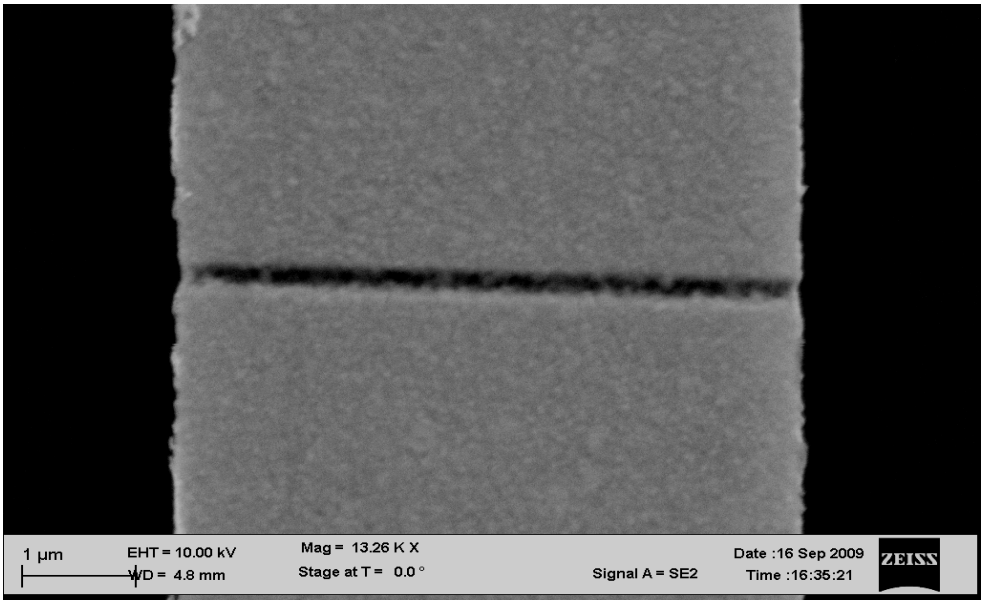

Figure 3.2 SEM micrograph of a break junction electrode after FIB scratch

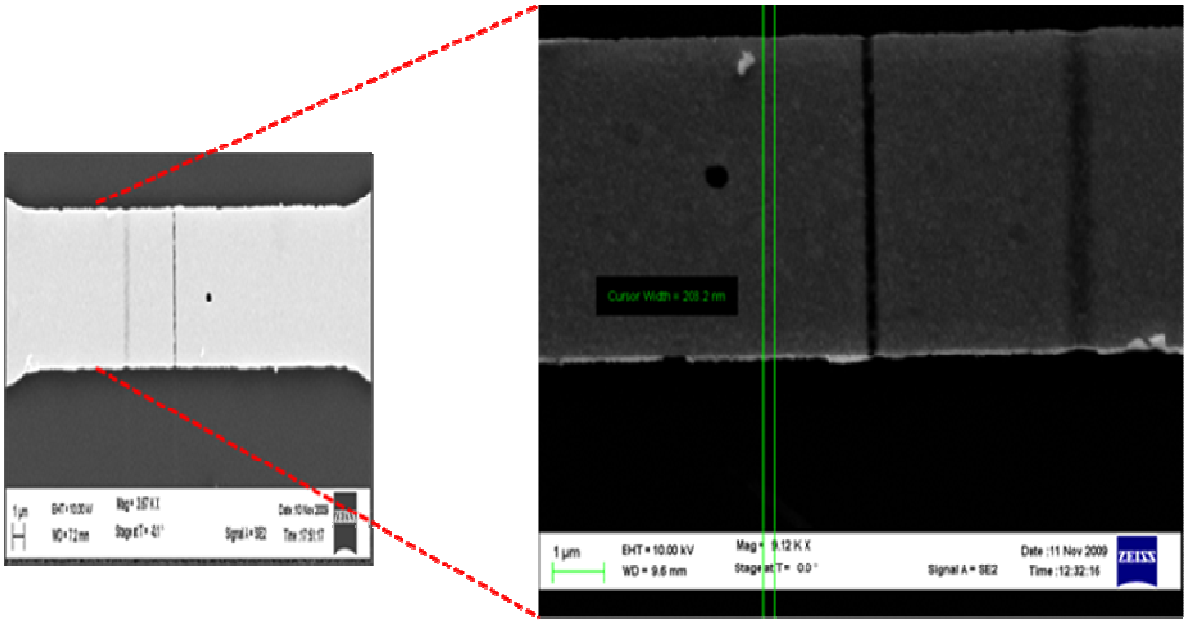

Figure 3.3 SEM micrograph showing the nanogap between the gold electrodes

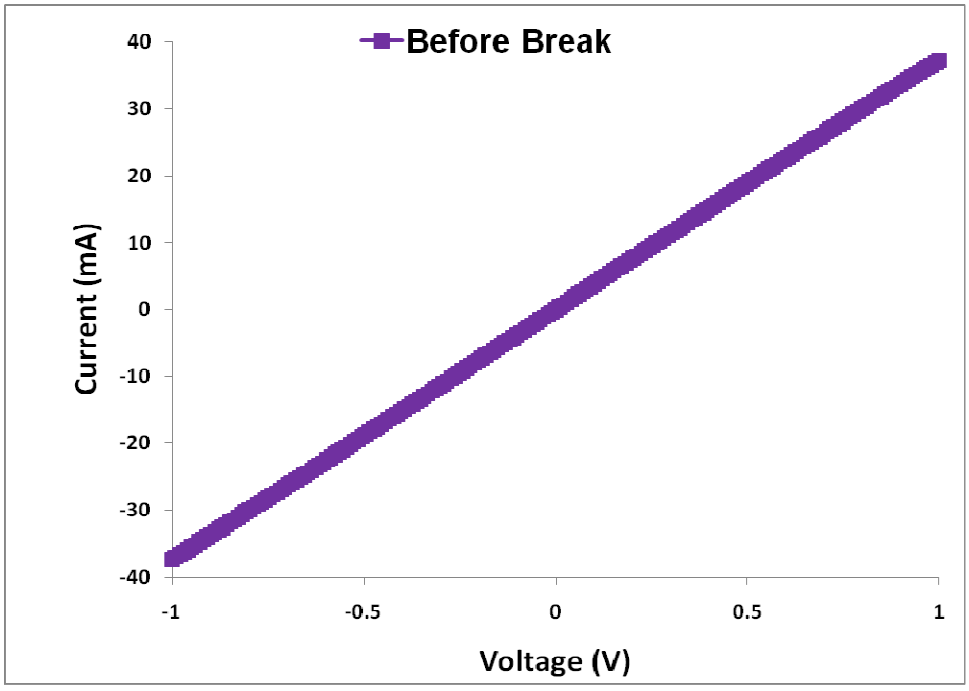

Figure 3.4 *I-V* measurements before break

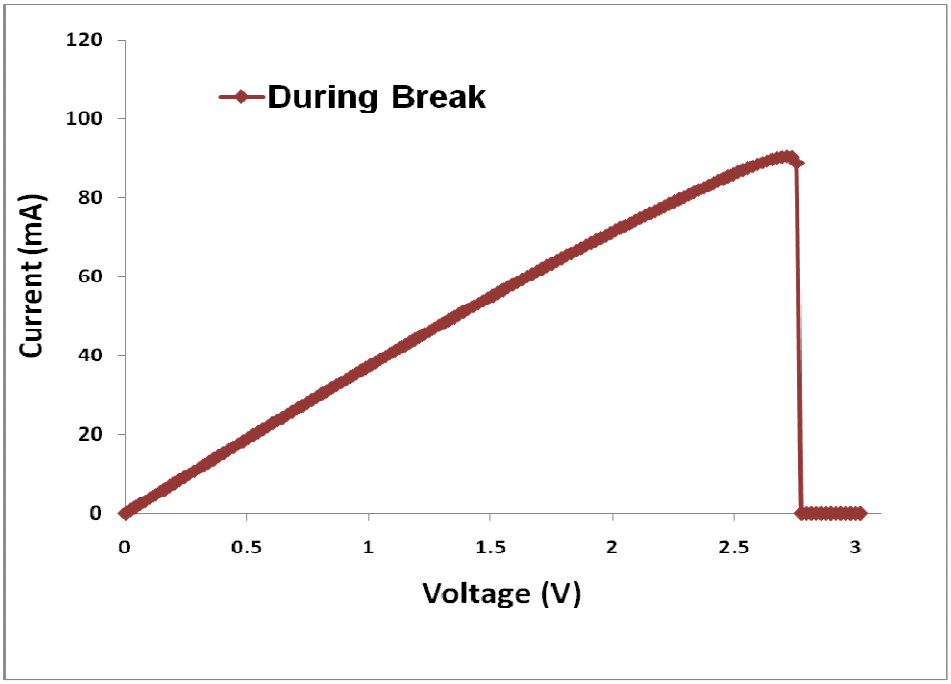

Figure 3.6 *I-V* measurements during break

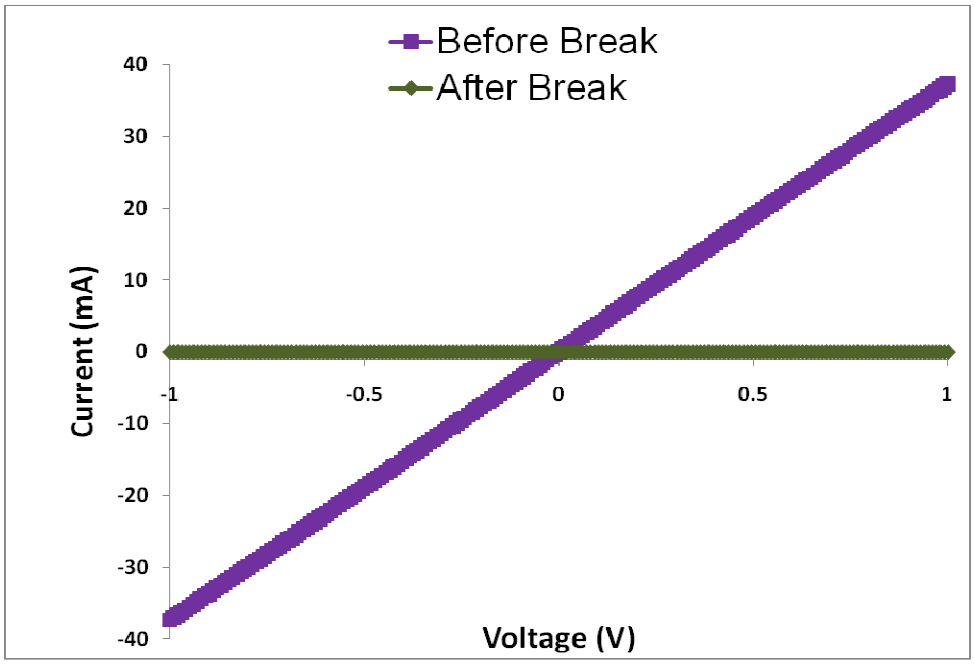

Figure 3.6 *I-V* measurements after break

3.4 Discussion

The results discussed in the previous section show that the break junctions were formed and characterized at each step. For the fabrication of the break junction chip, a specific mask design was decided upon. The nuances in the process of lithography had to be kept in mind when deciding the mask design. After the chip fabrication, it was initially proposed to break the electrodes by the application of a high voltage sweep. But upon completion of the process, it was seen that the gaps formed between the electrodes were in the micrometer range and were too large for use in a biological setting. This was attributed to the thickness of the gold electrode that was deposited on the silicon oxide surface. In order to overcome this problem, it was proposed to remove some of the gold material from the electrode. Towards this end, the FIB process was performed on the electrodes. This resulted in the removal of a thin layer from the gold electrode surface. After which the application of a high voltage sweep, resulted in gaps in the range of few hundred nanometers.

The principle of the break junction formation is that of electromigration. It is the phenomenon where the application of an external electric field causes a large current density in the wires. The electrons of the metal move under the influence of such fields; if a defect in the metal is encountered, the momentum of the electrons is transferred to the defect. Slowly, the momentum exchange becomes larger, resulting in the build-up of a force. This causes the atoms to move away from the defect culminating in the effective breakdown of the metal.

3.5 Conclusion

The fabrication of the break junction chip was done effectively. Nano-gaps of a few hundred nanometers were fabricated. The fabricated chips have wide applications in many diagnostic settings like in protein or cell detection. The break-junction chip is used for the detection of a cancer protein in Chapter 5.

CHAPTER 4

R2Bm DETECTION ON SILICON OXIDE CMOS CHIP

4.1 Introduction

R2Bm is a genetic element found in the organism *B. mori*. The double stranded DNA binds to a specific protein called the R2Bm protein. In this chapter the binding and detection of the dsDNA and the protein capture is discussed to demonstrate the working of a novel idea. A CMOS chip was used for the electrical measurements performed.

4.2 Fabrication of CMOS Chip

The CMOS chips were fabricated by the process of lithography in two steps. The first step involved the formation of the first layers. Titatnium/Gold (Thickness 50 Å/150 Å) metal pads 500 nm apart were made using e-beam lithography. Metal lift-off was performed to obtain well defined structures. The second step was optical lithography to fabricate the probing pads to contact the thin film electrodes.

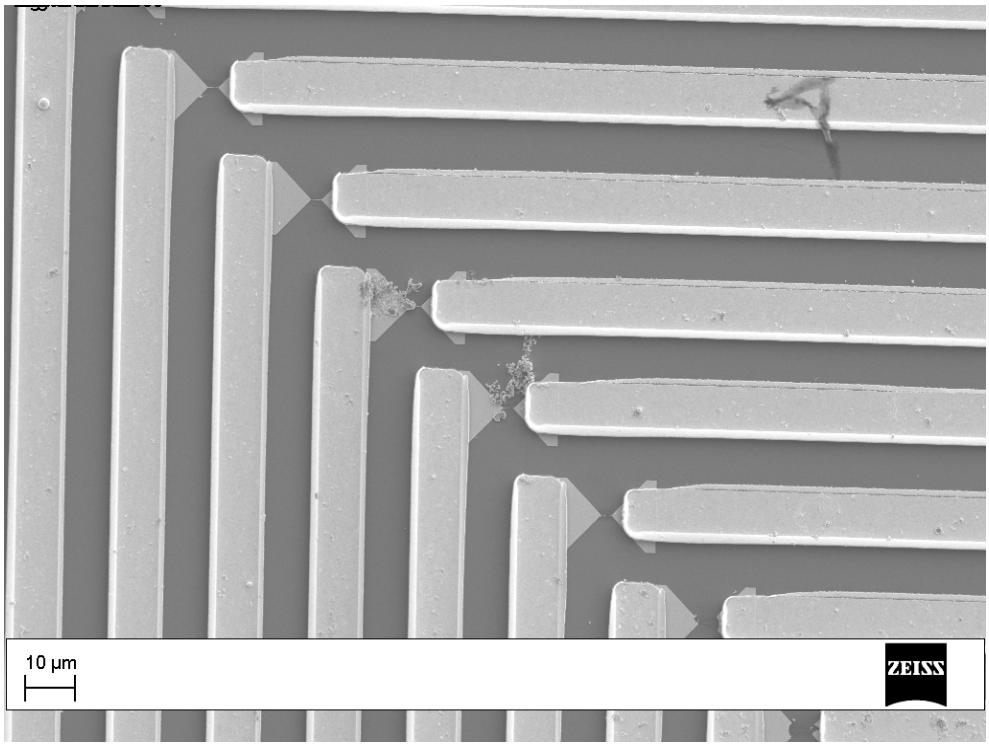

Figure 4.1 SEM micrograph of the CMOS chip used for protein detection

4.3 Attachment of dsDNA and Capture of Protein R2Bm on Silicon Oxide

The silicon chip was cleaned using UV Ozone plasma system. This resulted in hydrophilic SiO_2 surface. The attachment chemistry was performed in a nitrogen glovebox in a controlled environment, as reported previously [68]. Briefly, the chips were silanized in a 5% Aminopropyltrimethoxysilane (APTMS) solution (made with 19:1 methanol-de-ionized water) for over 12 hours. These were then washed with methanol, de-ionized water (DIW) and dried with nitrogen gas. The chips were immediately immersed in a Dimethylformamide (DMF) solution containing pyridine and p-phenylene diisothiocyanate (PDITC) overnight. The chips were sequentially washed with DMF and 1,2–dichloroethane and dried under nitrogen gas. The dsDNA sequence solution was prepared at a concentration of 1 pmole/µl and chips were immersed in it immediately. The chips were incubated overnight in order to facilitate the covalent attachment of the 3′-amino modified dsDNA with the PDITC cross linker molecules. The chips were again washed and dried under nitrogen. The unbound reactive groups from PDITC were deactivated by

immersing the chips in a solution of 6-amino-1-hexanol and diisopropylethylamine (DPEA) in DMF. The chips were then washed and dried with nitrogen gas.

The dsDNA used in these experiments was a 23 base-pair (bp) fragment of the ribosome gene that corresponds to the binding site of the R2Bm derived polypeptide [57]. In order to confirm that the purified R2Bm polypeptide is capable of binding to our short dsDNA, an electrophoretic mobility shift assay (EMSA) was run. Chips with covalently attached dsDNA were then incubated with 2.8 fmole/µl of R2Bm polypeptide for 30 minutes in binding buffer (50 mM Tris–HCl pH 8, 100 mM NaCl, 5 mM $MgCl_2$).

After the attachment of the dsDNA molecules on the silicon oxide surface, characterizations were performed to confirm the various surface modifications. Energy-dispersive X-ray spectroscopy (EDAX), contact angle and ellipsometry measurements were carried out at every step.

4.4 Optical Detection of DNA Attachment and Protein Capture

The presence of dsDNA immobilized on the silicon surface was confirmed by fluorescence measurements of Acridine Orange stain at 525 nm wavelength using Zeiss Confocal Microscope. The presence of the protein on the chip was initially confirmed by optical detection using fluorescent *Sypro Ruby Protein Blot* stain at 488 nm. The fluorescence intensity analysis was carried out using *ImageJ* software [69].

4.5 Electrical Detection of DNA Attachment and Protein Capture

The presence of the R2Bm protein captured by the dsDNA on the silicon surface was also confirmed by the electrical measurements. Direct Current (DC) measurements were performed on the CMOS chips after the immobilization of dsDNA and capture of the protein. The current-voltage (*I-V*) measurements were performed using Agilent Semiconductor Parameter Analyzer (4155C) on a probe station.

4.6 Results

The EDAX analysis was used to identify the elemental composition of the silicon surface as the different modifications were added. The data in Table 4.1 show the elemental increase in Carbon and Nitrogen after dsDNA immobilization. Control chips without dsDNA showed no change in carbon and nitrogen. The Contact angle measurements showed the silicon surface becoming hydrophilic after functionalization with APTMS and less hydrophilic when later modified with PDITC (Table 4.1).

Table 4.1. EDAX analysis – weight % of significant elements on chips with and without modifications

Element / **Chip Surface**	**C**	**N**	**O**
Clean Chip	0.2	8.2	320.4
PDITC	7.3	9.1	329.2
DNA	10.7	25.8	391.4

Table 4.2. Ellipsometry measurements

	Thickness	SD
Silicon dioxide	1203.66	2.18
APTMS	1213.35	7.32

The Ellipsometry measurements gave the thickness of the SAM of silane modification as shown in Table 4.2. The difference in the two thicknesses is around ~10 nm. The presence of dsDNA

immobilized on the silicon surface was confirmed by Acridine Orange (Fig. 4.2). Acridine Orange gives a green fluorescence when it interacts with dsDNA [70]. The Acridine Orange stain fluorescence obtained is a conclusive test result of the presence of dsDNA covalently attached on the surface of the CMOS chip.

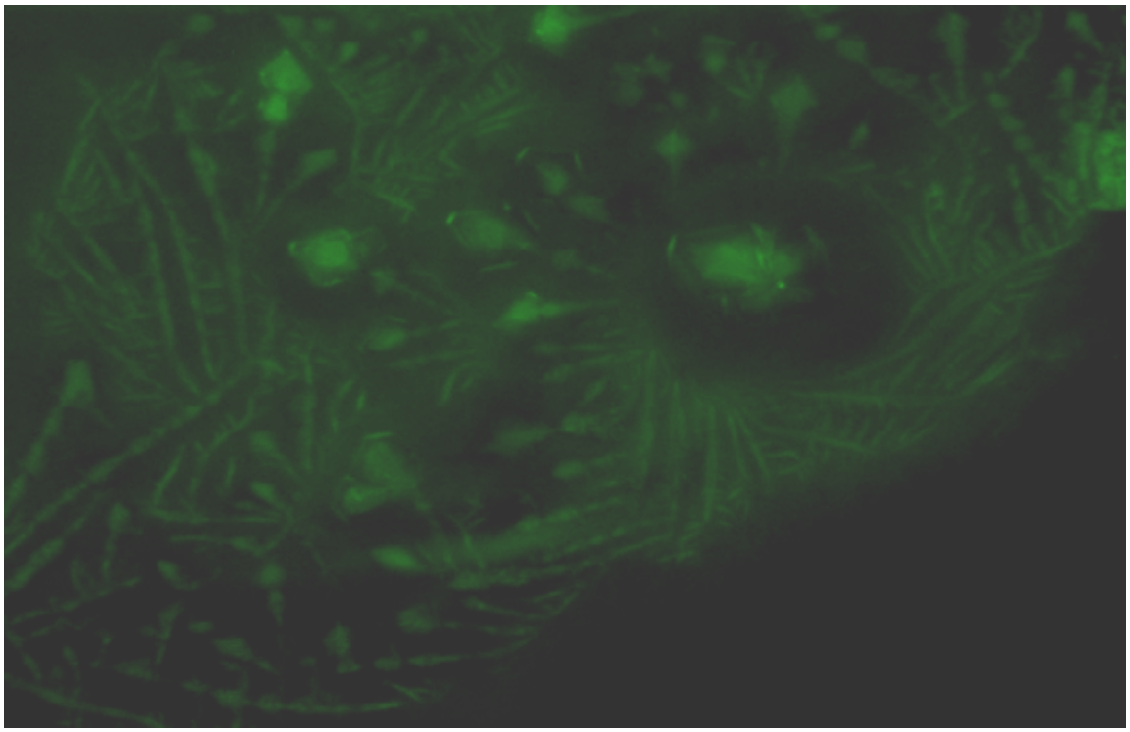

Figure 4.2 Silicon oxide chip showing dsDNA stained with acridine orange

Prior to functionalizing the chips, the polypeptide binding to the 23 bp dsDNA fragment was confirmed using electrophoretic mobility shift assay (EMSA)—a polyacrylamide gel electrophoresis based method of detecting protein-DNA interactions (Fig. 4.3).

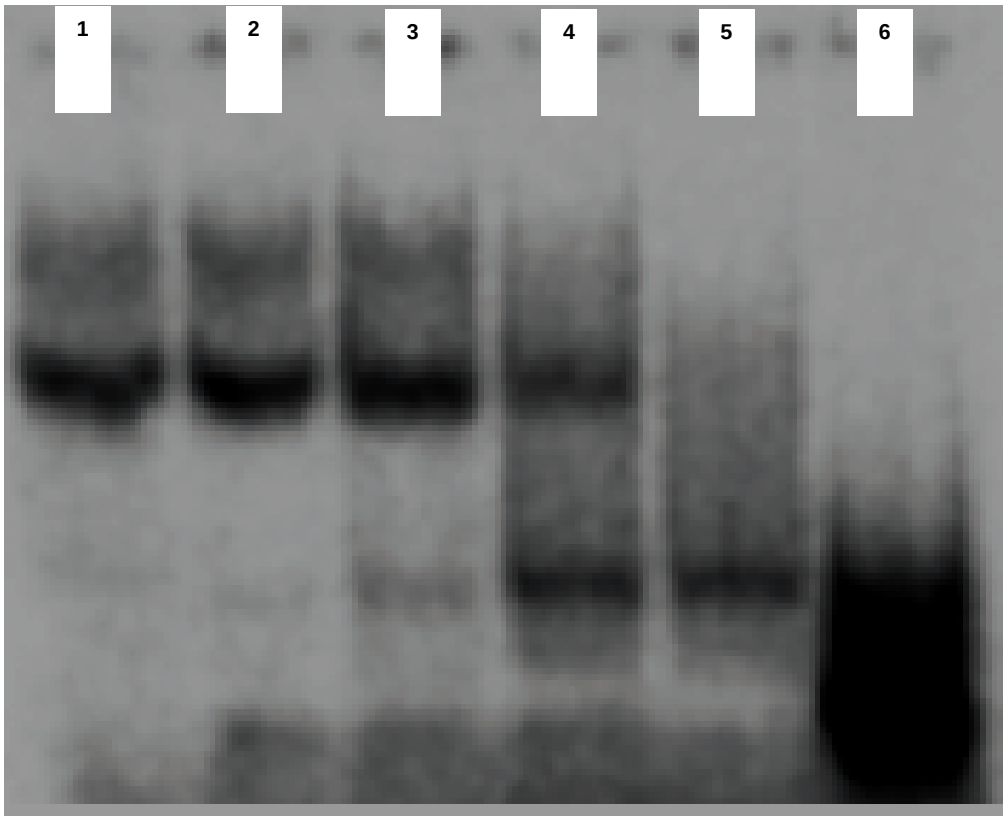

Figure 4.3 EMSA PAGE gel. The first 3 lanes (from L to R) 8.4 pmole, 2.8 pmole, 0.84 pmole, and 0.28 pmole protein, respectively, of R2Bm protein bound to 1 pM of dsDNA. The last two lanes (5 and 6) are dsDNA and ssDNA, respectively, in the absence of protein

Importantly, we can also see the peptide binding to the DNA on the functionalized chip. Figure 4.4 shows the protein stain Sypro Ruby data verifying the polypeptide binding to the DNA on the chip. Once the dsDNA immobilization on silicon chips and selective DNA-protein binding was verified with stains, the dsDNA and protein detection was done on nano-electrode CMOS chip, without any staining. Figure 4.5 shows the SEM micrograph of the nano-electrodes.

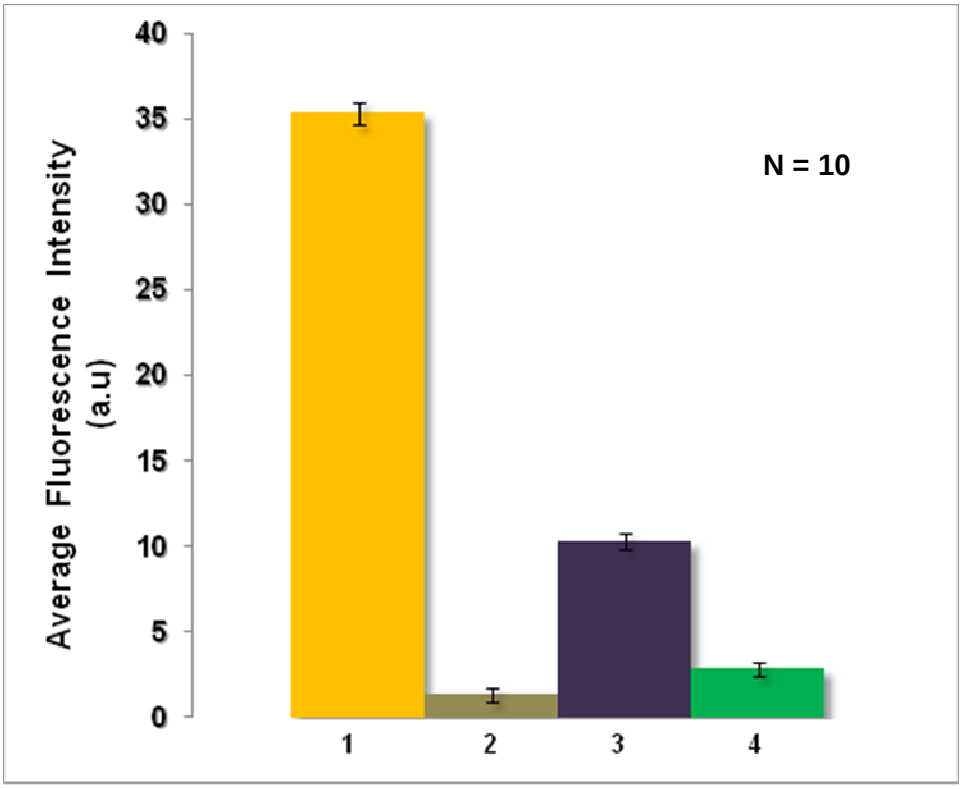

Figure 4.4 Sypro stain intensity measurements on chips with the following surface modifications: Chip 1 DNA & protein attached on chip; Chip 2: Only DNA immobilized on chip; Chip 3: Only APTMS modification on chip surface; Chip 4: Piranha cleaned chip surface (no biomolecule)

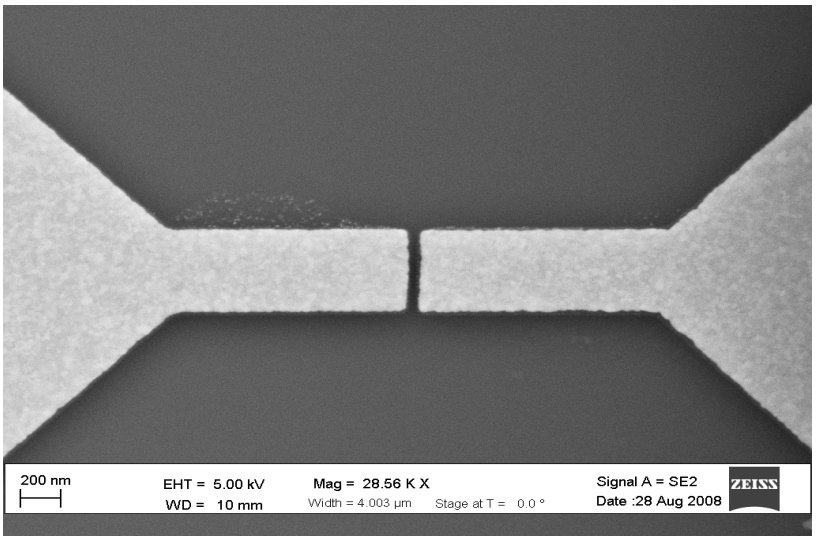

Figure4.5 SEM micrograph of the nano-electrodes

The current-voltage (*I-V*) measurements were performed using Agilent Semiconductor Parameter Analyzer (4155C) on a probe station. A chip without any biomolecules was used a control. The *I-V* data was recorded from -1 V to +1 V across the metal electrodes. The *I-V* data showed linear trend after the capture of proteins on surface immobilized dsDNA (Fig.4.6). The resistances of the devices ranged from few ohms to GΩ, indicating a varying number of proteins bridging the gaps between the electrodes.

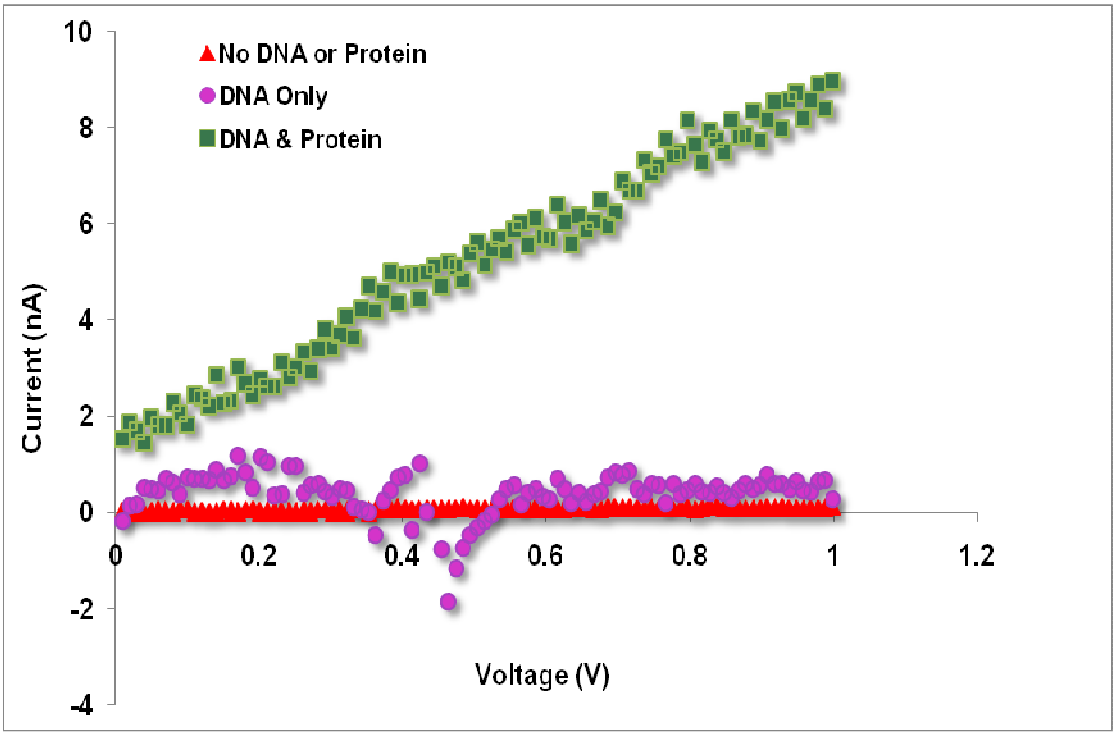

Figure 4.6 *I-V* measurements comparing current measured between nano-electrodes. Control data is red triangles and pink circles from chips with no surface bound dsDNA or protein and bound dsDNA only. The green squares show the *I-V* data for the chip with DNA and protein immobilized on the surface.

4.7 Discussion

The various results obtained show that the protein and the dsDNA did bind. But in the experiments leading to these results, many more details were also learnt. These are discussed in the following sections.

4.7.1 Surface Modification

The initial set of experiments for optical detection was performed on the surface of plain silicon oxide chips. A silicon wafer was thermally oxidized to get an oxide layer in the thickness of 1500 Å. The wafer was covered with a photo-resist. It was diced using a dicing-saw to dies of of 6 mm by 4 mm. Prior to using the chips for the experiments, the chips were immersed in acetone and placed in an ultrasonicator for 5 minutes to remove the photo-resist layer.

The different chemicals used in the surface modification process have specific roles to play in making the silicon surface ready for the attachment of the modified DNA molecule. Before beginning the surface modification process the chip surface was cleaned by UV ozone plasma. This cleaning also resulted in the chip surface becoming more hydrophilic and also introduced some –OH groups on the surface. The silicon present in the APTMS reacts with the –OH groups thus leaving the amine group available for reaction with PDITC linker modification. Of the two isothiocyanate groups present on the PDITC, one of those reacts with the APTMS and the other reacts with the amine group of the modified DNA molecule. The unreacted isothiocyanate groups were capped with 6-amino hexanol. This was done in order to prevent the attachment of the protein to the PDITC linker instead of the DNA. The protein was then flown in on the chips and the binding between the protein and the DNA was detected.

The EDAX, Ellipsometry and contact angle measurements were performed in order to confirm the different surface modifications. The results obtained from EDAX showed a higher concentration of carbon and nitrogen in the chips modified with PDITC and dsDNA when compared to a clean chip. The increased concentration of the two elements confirmed the presence of PDITC and DNA which have more nitrogen because of the chemical groups present in them. PDITC has more carbon and nitrogen in its phenylene and isothiocyanate groups. The dsDNA has more carbon and nitrogen because of the nitrogenous bases that make the DNA. The contact angle measurements were performed on chips at various stages of surface modification to observe the change in hydrophilicity. It was seen that after the piranha clean and modification with APTMS that introduces a silane layer on the chip, the chip surfaces

became more hydrophilic. But upon modification with PDITC, the hydrophilicity was seen to decrease. This could be explained by the presence of hydrophobic benzene rings on the PDITC molecule. The ellipsometry measurements indicated an increase in the thickness of the chip upon modification. It was also noted that different incubation times brought about different thicknesses.

The surface modifications were performed as described earlier. Through small changes in the protocol it was seen that the entire length of the experiment could be effectively shortened to a little over 2 days. The APTMS used to silanize the silicon surface was initially used at a concentration of 3% and the chips were incubated in it overnight. But later in order to shorten the effective experiment time, the APTMS concentration was increased to 5%. This reduced the incubation time to 4 hours.

4.7.2 DNA Attachment and Optical Detection

The DNA used in the experiment was a double stranded one. Two complementary single strands were purchased (Alpha DNA, Quebec, Canada) and annealed to form a double strand before use. The sequence of one of the strands was (5′-CTTAAGGTAGCAAATGCCTCGTC-3′). To this DNA strand an extension of 10 adenine residues were added at the 3’ end. At the end of the adenine nucleotide extension, an amine modification was included also at the 3’ end. The adenine extension was done to prevent the direct attachment of the dsDNA molecule on the silicon surface. The direct attachment of DNA on a surface prevents free movement which may have been an issue in protein capture. The amine extensions at the end of the dsDNA molecule were added to attach the DNA on the modified silicon surface. The amine group reacts with one of the isothiocyanate groups of the PDITC linker molecule.

The DNA hybridization is a process where two strands of DNA are heated to their denaturation temperatures wherein they form single strands and slowly cooled to reform the double stranded structure. This is a technique that is commonly used to study the relation between DNAs of different origin. The hybridization reaction was performed between the two single strands in order to obtain the complete double stranded structure. The process was performed in an STE hybridization buffer containing

predetermined concentrations of TRIS, EDTA (Ethylenediaminetetraacetic acid) and salt. The whole mixture was heated to 70 ℃ and allowed to cool to room temperature. After cooling, the solution was added on the chip for the attachment of the double stranded DNA. The formation of the dsDNA through hybridization is dependent on numerous factors. The most important among the are the melting temperature of the participating strands and the hybridization temperature and the ionic strength of the buffer solution.

The attachment of the dsDNA on the silicon surface had some issues that were addressed. It was noticed that when experiments were performed in containers and glassware that were not autoclaved, the DNA attachment did not occur. This was attributed to the presence of DNase on the glassware. DNase is enzyme that acts on DNA molecule and degrades these. The high temperature of autoclaving degrades the enzyme, thus glassware becomes compatible for DNA experiments.

After the attachments were performed, in order to confirm the presence of dsDNA on the silicon surface, acridine orange staining was performed. Acridine orange is an inorganic stain used to identify nucleic acids. It can penetrate the cell membrane and bind to the nucleic acid inside. A few iterations were carried out to optimize acridine orange concentration for best staining results. It was seen that if the concentration of the stain was low, the DNA molecules were not visible, and if the concentration was high, the background fluorescence from the control chips would saturate the image thus losing differentiation between control and real samples. Acridine Orange gives a green fluorescence when it interacts with dsDNA [70]. It has an excitation maximum at 502 nm and an emission maximum at 525 nm when detecting dsDNA. When detecting RNA, which are single stranded molecules, the excitation maximum of the stain shifts to 460 nm and the emission maximum is at 650 nm. The acridine orange stain bears a positive charge and binds electrostatically with the dsDNA. Electrostatic interactions with non-specific polyanions was avoided by using a very low concentration of the stain (0.2% v/v) and including other cations like Mg^{2+}, Na^{+} in the buffer solution that would compete for the binding with the dsDNA [71].

The fluorescent images were analyzed using the *ImageJ* software. For every chip, 2 to 3 images were taken. From every image 10 data points were randomly chosen and analyzed.

4.7.3 Protein attachment and Optical Detection

The R2Bm protein was made in-house [57]. The R2Bm derived polypeptide sequence is MGSSHHHHHHSSGLVPRGSHMRTGDNPTVRGSAGADPVGQDAPGWTCQFCERTFSTNRGLGVHKRR AHPVETNTDAAPMMVKRRWHGEEIDLLARTEARLLAERGQCSGGDLFGALPGFGRTLEAIKGQRRREPY RALVQAHLARFGSQPGPSSGGCSAEPD. The protein has the zinc finger and Myb motifs that bind to the dsDNA sequence as described earlier [57, 61].

Prior to detecting the presence of the protein on the silicon chip, it was required to confirm the binding of the R2Bm protein with the fragment of the dsDNA that was used. Towards this goal, an EMSA (Electrophoretic Mobility Shift Assay) was performed. An EMSA gel is an electrophoresis technique used to study protein – DNA interactions. For the assay, half the single strands of DNA were radio-labeled with α-P^{32}CTP which is the nitrogenous base cytosine with a radioactive phosphate group. After radio labeling, the two strands of DNA were annealed (as described earlier). The EMSA gel was then run, with different concentrations of the protein in different lanes. The DNA-protein interactions were observed. It was seen that the of protein was able to bind to the DNA at 0.28 pmole concentration as seen in figure 3.3.

For the binding of the R2Bm protein with the dsDNA on CMOS chips, the protein was made up to a concentration of 2.8 fmole/μL in phosphate buffered saline with a low concentration of Mg^{2+}. The presence of the Mg^{2+} ions helps in shielding the negative charge of the dsDNA. The negative charge on the dsDNA molecule is because of the phosphate backbone. The shielding charges help binding the two negatively charged single strands through electrostatic attractions. The binding between the protein and DNA was allowed to proceed for 45 minutes. The binding between protein and DNA was initially confirmed by optical detection using a fluorescent microscope at 488 nm wavelength. A polypeptide selective stain, *Sypro Ruby Protein Blot* stain was used. The Sypro Ruby stain is a ruthenium based stain

that detects the amino acids lysine, arginine and histidine [72]. The R2Bm protein has these amino acids in its sequence and hence could be detected by the stain when viewed under a fluorescent microscope. It was noted that during the optical detection experiments, the fluorescence staining on the chips was the brightest and freshest only when imaged soon after the staining. If the stained chips were imaged after a few hours, a decrease in the fluorescent intensity was noted. As the results are based on the fluorescent intensity measured from the chips, it is required that the chips be imaged right after staining.

The images were analyzed using the *ImageJ* software. For every chip, 2 to 3 images were taken. From every image 10 data points were randomly chosen and analyzed.

4.7.4 Electrical Detection of dsDNA and R2Bm protein

The CMOS chip was fabricated with patterned gold pads that were set at a width of a few nanometers. Before the surface modifications were performed on them, the gold pads had to be broken such that the gap in between them was in the order of a few hundred nanometers. In order to accomplish this, the gold pads were biased ramping 0 to 5-10V. The electro migration caused by the formation of break junctions in the order of a few hundred nanometers. The nano-gaps exposed the silicon dioxide layer beneath thus giving room for the dsDNA attachments to occur.

The CMOS chip with the brokens junction was cleaned with UV ozone plasma for a few minutes and the attachment chemistry was performed on it. After the attachment of DNA and DNA-protein binding, the *I-V* data from -1 V to +1 V was measured across the gold electrodes that were around 500 nm apart. In all, *I-V* data from 120 devices were measured in each case. As a control, a chip with no surface modifications was used and the *I-V* data was also measured. A linear trend in the *I-V* data was noticed after the capture of proteins by the immobilized dsDNA. The resistance was seen to decrease from GΩ to MΩ. The linear trend in the *I-V* data pointed towards the conducting behavior of the protein, while the control chip showed the behavior of an open circuit before and after functionalization. The current measured in the case of the functionalized chips can be explained by Simmons' formula. It explains the

tunneling current seen in a system with nanogap electrodes with an insulator between them. Simmons' formula can be given by:

$$J = (\frac{\alpha}{\delta_z^2})\{\bar{\phi}\exp(-\mathrm{A}\delta_z\sqrt{\bar{\phi}}) - (\bar{\phi} + eV)\exp[-\mathrm{A}\delta_z\sqrt{\bar{\phi} + eV}]\}$$

where $\alpha = e/(4\pi^2\beta^2\mathrm{h})$, A=2β, $\bar{\phi}$ is the average barrier height relative to Fermi level of the negative electrode, δ_z is the barrier width, and eV represents the applied voltage across the nanoelectrodes. B is the dimensionless correction factor, e and m are the charge and mass of electron respectively, and $\hbar$ is Dirac's constant. At small voltages when $\bar{\phi} \gg eV$, the Simmons' formula simplifies as $J = (\gamma\sqrt{\bar{\phi}V}/\delta_z)\exp(-A\delta_z\sqrt{\bar{\phi}})$, where $\gamma = (e\sqrt{2m})/(4\beta\pi^2\mathrm{h}^2)$. In the case of small voltages, the barrier height $\bar{\phi}$ becomes independent of the applied voltage and the tunneling current becomes linearly dependent only on the applied voltage. The tunneling current characteristic can thus be modeled as two electrodes with high resistance between them. As the DNA and DNA-protein complex immobilize between the electrodes, the electrons find a path of lower barrier and hence tunnel current more efficiently.

During the *I-V* measurements there was a concern that the DNA immobilized on the chip surface and protein captured by it may degrade as the measurements were done in a dry state. Usually the electrical measurements are performed in the solution state, measuring the impedance from the devices. But, in this case, the measurements were in a dry state. The chips were dried with nitrogen gas as it is an inert gas and will not affect the outcome of the experiment in any manner. In order to avoid denaturation of the protein and the DNA molecules on the chip, the *I-V* probe measurements were completed within two days. It has to be kept in mind that once the protein has been attached on the surface of the chip, the detections will have to be performed as soon as possible.

4.8 Conclusion

The R2Bm dsDNA was immobilized on the CMOS chip and the protein was captured by it. The protein capture was optically and electrically detected. The concentration of 2.8 fmol detected by the mode of detection is very competitive and compares to the commercially available and reported protein detection limits. The results obtained further validate the novel idea and design proposed for protein detection.

CHAPTER 5

EGFR DETECTION ON SILICON OXIDE CMOS CHIP

5.1 Introduction

EGFR is a biomarker protein for many cancers and other diseases. This section describes the electrical detection of EGFR using the EGFR RNA aptamer as the selective agent. Aptamers are nucleic acids or peptide molecules that are selected for their highly specific binding to small target molecules. They are selected through a process called SELEX. The electrical detection of a cancer protein with the use of CMOS chips is described here.

5.2 Fabrication of CMOS Chip

A CMOS chip was fabricated by the processes described in Chapter 3. The gold pads of the chip were made using optical lithography. Break junctions were made from these gold pads by electromigration. The junctions were spaced at a few nanometers. The *I-V* data from each of the electrodes pairs was recorded before and after the breaking was done. Scanning electron microscopy (SEM) of every electrode pin was taken and the nanogaps between the electrode pins were measured.

5.3 Attachment of Aptamer and Capture of Protein on Silicon Oxide

The silicon chip was cleaned using UV Ozone plasma system. This also resulted in hydrophilic SiO_2 surface. The attachment chemistry was performed in a nitrogen glovebox in a controlled environment, as reported previously [68]. Briefly, the chips were silanized in a 5% APTMS solution (made

with 19:1 methanol-DIW solution) for over 4 hours. These were then washed with isopropanol, DIW and dried with nitrogen gas. The chips were immediately immersed in a DMSO solution containing pyridine and PDITC overnight. The chips were washed with ethanol, DIW and dried under nitrogen gas. The single stranded DNA (ssDNA) sequence solution was prepared at a concentration of 1 μM and chips were immersed in it immediately. The chips were incubated overnight in order to facilitate the covalent attachment of the 3′-amino modified ssDNA with the PDITC cross linker molecules. The chips were again washed with ethanol and dried under nitrogen. To the single stranded DNA with an amine modification that was bound on the silicon surface, the RNA aptamer with an extension complementary to the bound single stranded DNA was attached. The chips were incubated for 2 hours. They were then washed and dried with nitrogen gas.

The ssDNA used in these experiments was a short sequence of oligonucleotides, with an amine modification at the 3' end. The RNA aptamer was developed by The Ellington Lab at UT Austin. The RNA aptamer had a short extension that was complementary to the amine modified ssDNA. Along with the RNA aptamer, a mutated RNA sequence was also used. This RNA sequence had a mutation which prevented it from recognizing the EGFR protein. Hence, it would not bind to the EGFR protein.

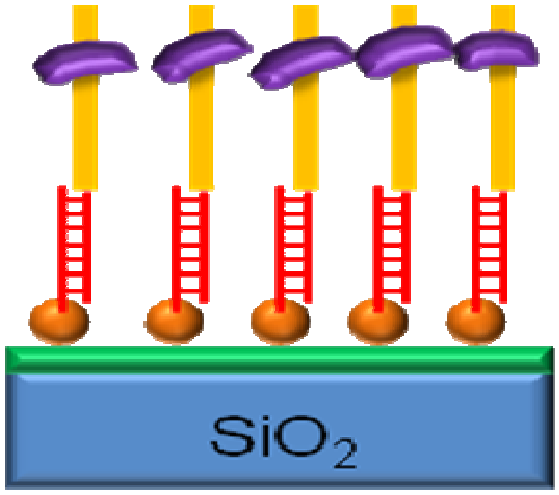

Figure 5.1 Schematic representation of RNA aptamer binding and protein capture on the silicon oxide surface

Chips with the attached RNA aptamer were then incubated with 50 ng/µl of EGFR protein for 45 minutes in PBS with 25 mM Mg^{2+}.

5.4 Optical Detection of Aptamer and Protein Capture

The attachment of the ssDNA and the RNA aptamer was confirmed by optical detection initially. This was done by the use of the inorganic stain, acridine orange. A concentration of 5 mg/mL was used in the staining experiments. The chips were incubated with the stain for 30 minutes. In order to confirm the capture of the EGFR protein, *Sypro Ruby Protein Blot* stain was used. The staining process was done for 30 minutes. The chips were analyzed using a fluorescent microscope. The images were analyzed using the *ImageJ* software. For every chip, 2 to 3 images were taken. From every image 10 data points were randomly chosen and analyzed.

5.5 Electrical Detection of Aptamer Attachment and Protein Capture

Towards the electrical detection of the protein, a voltage sweep of -1 V to +1 V was applied across the electrodes. The change in current was recorded.

5.6 Results

The analysis of the images taken after the fluorescent staining confirmed the presence of the RNA aptamer and the EGFR protein on the surface of the chip.

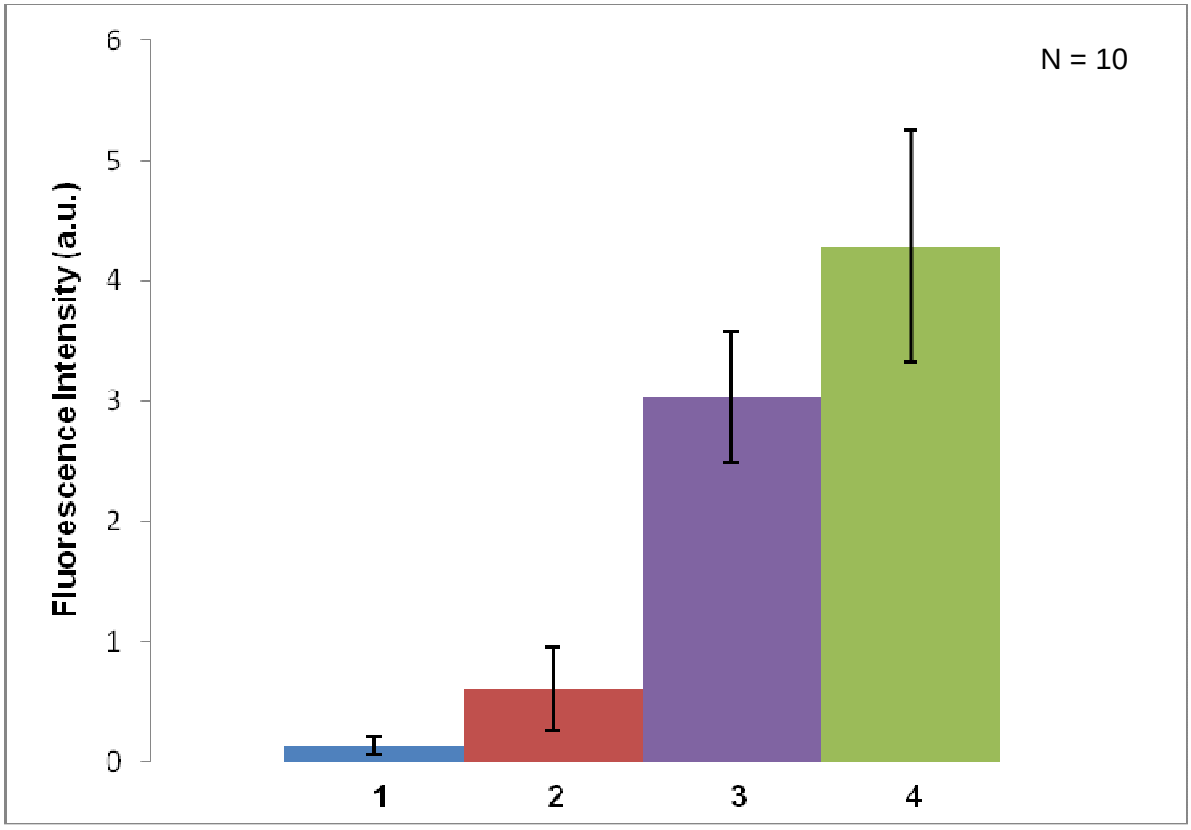

Figure 5.2. Acridine orange staining on silicon oxide chips to confirm the presence of RNA aptamer on the chip surface. From L to R: Chip 1 – Control chip with APTES modification stained with acridine orange; Chip 2 – Control chip with PDITC modification stained with acridine orange; Chip 3 – Chip with mutant RNA immobilized; Chip 4 – Chip with RNA aptamer immobilized

Results obtained from the Sypro staining confirmed the capture of the EGFR protein by the RNA aptamer and not the mutated RNA as seen in figure 5.3.

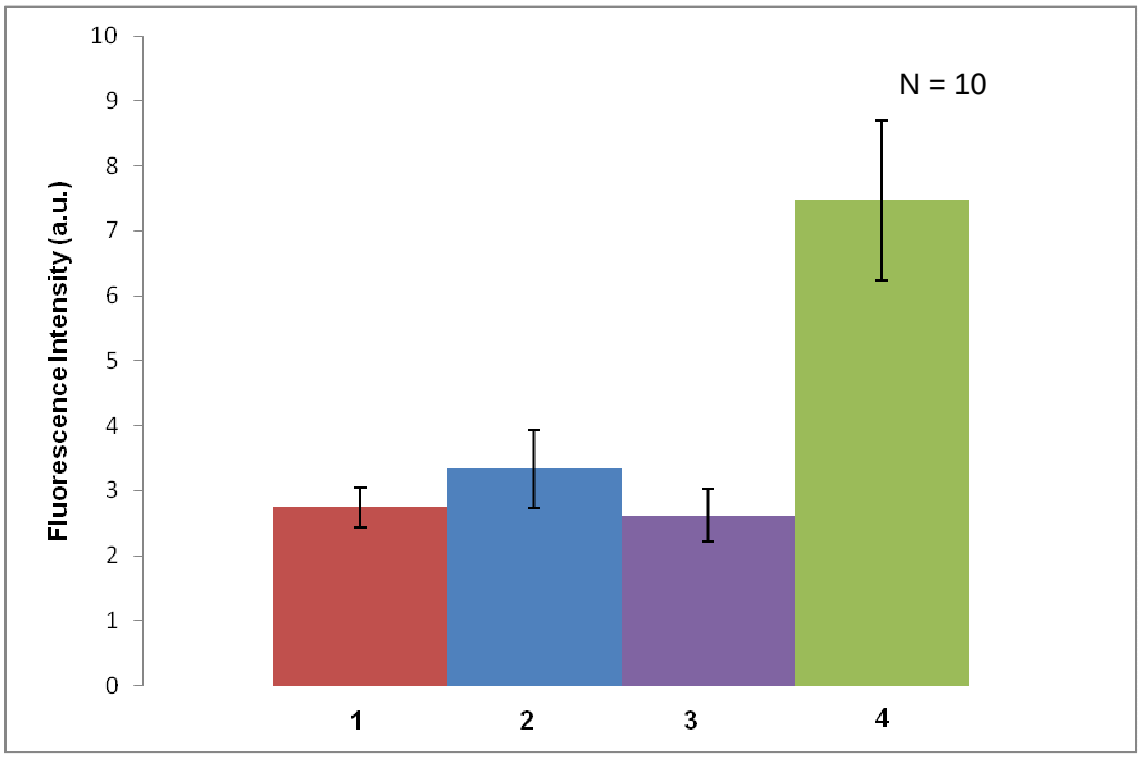

Figure 5.3. Sypro staining on silicon oxide chips to confirm the protein capture by the RNA aptamer. From L to R: Chip 1 and 2 – chips with APTES and PDITC modifications and protein; Chip 3 – Chip with Mutated RNA immobilized and EGFR protein; Chip 4 – Chip with RNA aptamer immobilized with EGFR protein captured

The electrical data from the protein detection give room for better results but a representative data shows the increase in current measured across the electrodes when the aptamer and protein were present.

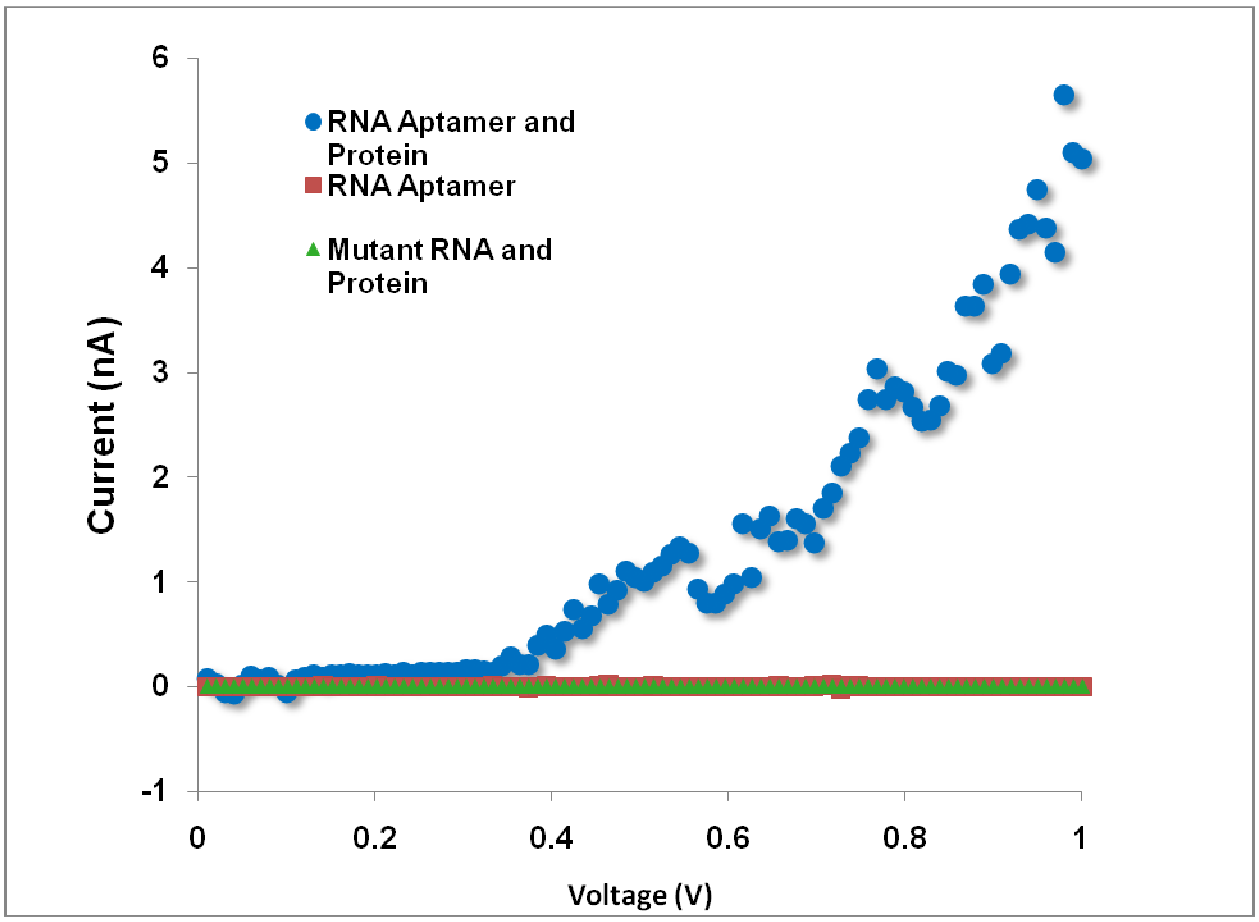

Figure 5.4 *I-V* measurements comparing current measured between nano-electrodes. Control data is green triangles and red sqaures from chips with only the RNA aptamer and mutant RNA with protein. The blue circles show the *I-V* data for the chip with RNA aptamer and protein immobilized on the surface.

5.7 Discussion

5.7.1 Surface Modification

The surface modifications were performed based on the same principles of chemistry as explained earlier in Chapter 4. In these set of experiments a few changes were made to the protocol to ensure that the RNA was kept intact throughout the process. The de-ionized water used was treated with Diethyl pyrocarbonate (DEPC), to inactivate Ribonucleases (RNases). RNases are enzymes that act on RNA and degrade them. RNases are very stable enzymes that are not deactivated by autoclaving or

chemicals. RNases produced in almost every secretion of the body and can find its way to the glassware and other accessories used during the experiments. Hence, DEPC treated water was used to minimize the risks of RNase action.

The initial set of experiments for optical detection was performed on the surface of plain silicon oxide chips. A silicon wafer was thermally oxidized to get an oxide layer in the thickness of 1500 Å. The wafer was covered with a photoresist. It was diced using a dicing-saw to chips with a dimension of 6X4 mm. Prior to using the chips for the experiments, the chips were immersed in acetone and placed in an ultrasonicator for 5 minutes to remove the photoresist layer.

5.7.2 RNA Aptamer attachment and Protein Capture

The ssDNA fragment was first attached on the silicon oxide surface. Hybridization was carried out on the surface of the chip rather than in solution. Initial experiments were performed without the use of the ssDNA. The RNA with a short extension was used in the experiments. Upon confirmations with the acridine orange staining, it was seen that the RNA aptamer was indeed present on the chip surface. The EGFR protein was also captured by it. This is clearly seen in the following graphs in the figures 5.3 and 5.4. The experiments had to be repeated however, as the reactions and chemistry leading to the binding of the RNA aptamer and protein capture could not be explained effectively. It is supposed that the nitrogen groups in the RNA molecule formed bonds with the isocyanate groups in the PDITC surface modification.

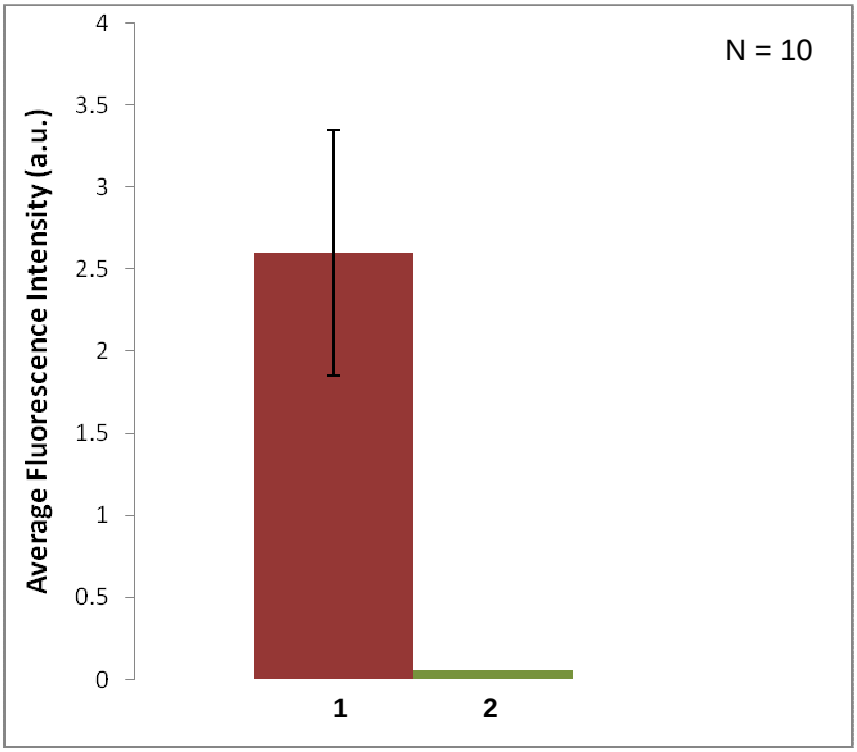

Figure 5.4. Acridine orange staining on siliocn oxide chips confirming the immobilization of RNA aptamer without modification (Chip 1) when compared to a control (Chip 2)

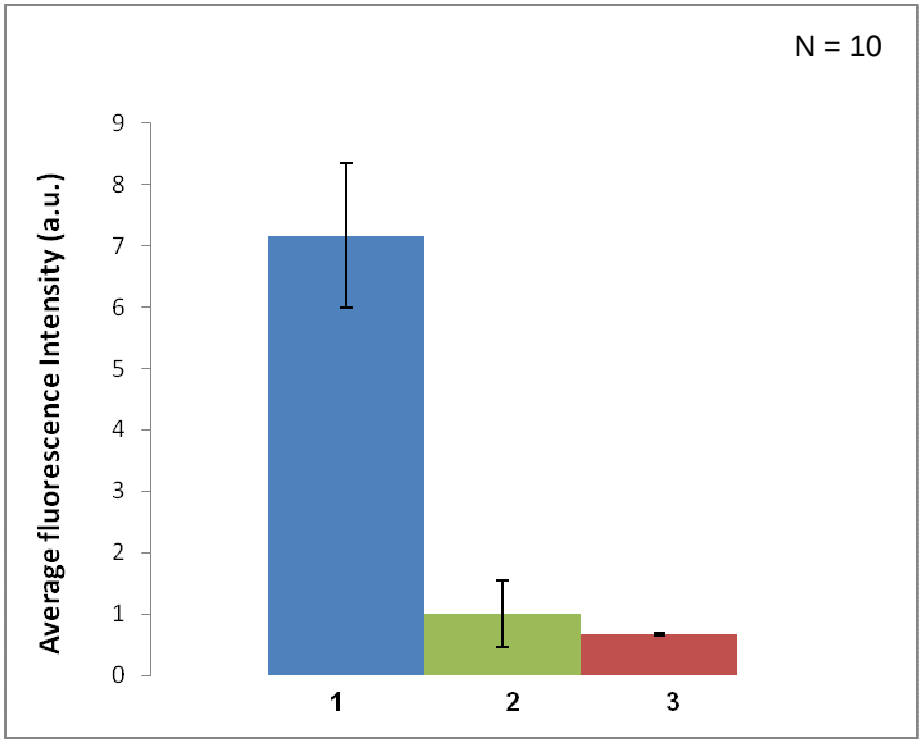

Figure 5.5 Sypro Ruby protein blot staining on silicon oxide chips confirming the capture of EGFR protein by RNA aptamer without modification (Chip 1) when compared to a controls (Chip 2 and 3)

The experiments were repeated with minor changes to increase the binding efficiency. The solvent used was changed from DMF to Dimethylsulfoxide (DMSO). DMSO was used as it is a solvent commonly used with DNA attachment chemistries. DMSO is also very effective when used in hybridization experiments. At the step of DNA-DNA hybridization, a humid atmosphere was required. In order to provide a conducive atmosphere, the chips were placed in a hybridization chamber and placed in a water bath at 37 ℃. It was observed that with th e change in protocol and experiment environment, better results were obtained. A few runs of the experiment had to be discarded, because in one case, the APTES incubation time was so short that efficient DNA attachment did not occur. This was rectified by increasing the APTES inubation time to over 5 hours. In another case, detection of the bound DNA was not possible as the acridine orange concentration used was very low. This was corrected by increasing the concentration by one order. In a third run of the experiment, due to faulty sealing of the hybridization chamber, samples were lost due to water leakage into the chamber. This was corected by double-

checking every section of the chamber for effective sealing. Once the nucleic acids were attached and detected, and the protein was flowed through, the protein was not detected by the optical analysis. Upon checking the

The sequence of the RNA aptamer that captures the EGFR protein is 5'-GGC GCU CCG ACC UUA GUC UCU GUG CCG CUA UAA UGC ACG GAU UUA AUC GCC GUA GAA AAG CAU GUC AAA GCC GGA ACC GUG UAG CAC AGC AGA GAA UUA AAU GCC CGC CAU GAC CAG-3'. The sequence of the mutant RNA used is 5'-GGC GCU CCG ACC UUA GUC UCU GUU CCC ACA UCA UGC ACA AGG ACA AUU CUG UGC AUC CAA GGA GGA GUU CUC GGA ACC GUG UAG CAC AGC AGA GAA UUA AAU GCC CGC CAU GAC CAG-3'. The underlined part represents the RNA sequence that binds to the 3' amine modified single stranded DNA fragment. The sequence of the DNA oligonucleotide is 5'-CTG GTC ATG GCG GGC ATT TAA TTC-3'. In order to prevent denaturation by RNases, The Ellington Lab introduced modifications to the pyrimidines at the 2' end. The modification was introduced to both the mutant RNA and RNA aptamer as well. This modification along with the use of DEPC treated water reduced the chances of denaturation by RNases.

5.7.3 Optical Detection of Aptamer and Protein Capture

The RNA aptamer that was attached on the silicon oxide was detected by the acridine orange stain. As RNA is a single stranded nucleic acid, the fluorescence measurements were taken at an excitation maximum wavelength of 460 nm and the emission maximum wavelength of 650 nm. Because of the presence of the double stranded structure close to the surface, it was expected to see some fluorescence when analyzed at emission wavelength of 525 nm when excited at a wavelength of 502 nm. Fluorescence images of double stranded structures were also obtained confirming the presence of the double stranded oligos.

The capture of the EGFR protein by the RNA aptamer and not the mutant RNA confirmed the selectivity of the RNA aptamer. The graph on figure 5.4, confirms the capture of the protein by the

aptamer. The fluorescence intensity measured is double than the control chips. The selective binding of the aptamer is attributed to the folding and secondary structures of the RNA molecule. These changes even with the slightest change in the RNA sequence. This is evident in the mutant RNA not recognizing and binding the EGFR protein. The presence of the protein on the chip surface was confirmed by imaging the Sypro stain under a fluorescent microscope at a wavelength of 488 nm.

5.7.4 Electrical Detection of Aptamer and Protein Capture

The graph in Fig. 5.3 shows the increase in current after the binding event of the RNA aptamer and EGFR protein. Though this gave an evidence of the presence of protein on the chip surface, there was not a high yield recorded in the experiment. The measure of current across the chip with only the RNA and the chip with mutant RNA and aptamer was recorded to be in the same nA range. This could be due to the non-binding event between the mutant RNA and the EGFR protein. As only a limited number of experiments have been performed, it would be too early to comment on the exact event as yet.

5.8 Conclusion

The results obtained from the experiments of electrical detection in this section support the initial goal of electrically detecting a cancer protein. A protein concentration of 50 ng/μL was detected by a label-free process. In the future, experiments will be designed to analyze the different protein concentrations and the currents recorded against them for a particular RNA aptamer concentration and vice versa.

CHAPTER 6

RESONANCE SENSING OF EGFR DETECTION ON TITANIUM OXIDE SURFACE

6.1 Introduction

The detection process described in this chapter is based on guided-mode resonance. Guided-mode resonance occurs when an incident wave is phase matched to a leaky waveguide mode supported by the waveguide grating structure. Because of the two polarizations that can be detected by the technology, real-time measurements of binding events are possible.

6.2 Attachment of Aptamer and Capture of Protein on Titanium Dioxide

The attachment of the aptamer was performed on two different surfaces of titanium dioxide for different modes of analysis. In order to confirm the surface chemistry and the immobilization of the nucleic acid on the titanium dioxide surface, a silicon wafer was coated with a layer of titanium dioxide. This wafer was diced using a dicing-saw to dies of the size 6 mm X 4 mm. The attachment process performed on the chip is given below.

The chips were cleaned with the piranha process, using sulfuric acid and hydrogen peroxide in equal ratios. This also resulted in hydrophilic SiO_2 surfaces. The attachment chemistry was performed in a nitrogen glovebox in a controlled environment, as reported previously [68]. Briefly, the chips were silanized in a 5% APTES solution (made with 19:1 methanol-DIW solution) for over 4 hours. These were then washed with isopropanol, DIW and dried with nitrogen gas. The chips were immediately immersed in a DMSO solution containing pyridine and PDITC overnight. The chips were washed with ethanol, DIW and dried under nitrogen gas. The single stranded DNA (ssDNA) sequence solution was prepared at a concentration of 1 μM and chips were immersed in it immediately. The chips were incubated overnight in order to facilitate the covalent attachment of the 3′-amino modified ssDNA with the PDITC cross linker

molecules. The chips were again washed with ethanol and dried under nitrogen. To the single stranded DNA with an amine modification that was bound on the silicon surface, the RNA aptamer with an extension complementary to the bound single stranded DNA was attached. The chips were incubated for 2 hours. They were then washed and dried with nitrogen gas. Chips with the attached RNA aptamer were then incubated with 50 ng/µl of EGFR protein for 45 minutes in PBS with 25 mM Mg^{2+}.

The ssDNA used in these experiments was a short sequence of oligonucleotides, with an amine modification at the 3' end. The RNA aptamer had a short extension that was complementary to the amine modified ssDNA. Along with the RNA aptamer, a mutated RNA sequence was also used. This RNA sequence had a mutation which prevented it from recognizing the EGFR protein. Hence, it would not bind to the EGFR protein when it was flowed in.

The titanium dioxide chips were then analyzed for the presence of the RNA aptamer and the captured EGFR protein by using the fluorescent dyes, acridine orange and Sypro Ruby Protein Blot stain respectively.

The second set of attachment chemistry was performed on titanium dioxide coated polyacrylate plates. The same attachment chemistry as mentioned earlier in this section was followed on the plate as well. The detection of the RNA aptamer and protein binding was confirmed by analyzing the resonance waves produced. The resonance shift measurements were performed in a 96 well micro titer plate. Each well was assigned a specific surface modification. The measurements were performed in the Vides Benchtop Plate Reader. These measurements were performed in real-time. Thus measurements were performed as the molecules bound to the different chemical groups on the surface. These surface modifications were closely monitored.

6.3 Results

6.3.1 Optical Detection of Aptamer Immobilization and Protein Capture

The figures 6.1 and 6.2 show the fluorescence intensity measurements from the staining experiments. There is a marked increase in the intensity measured from the chips with the RNA aptamer and EGFR protein when compared with the control chips. The fluorescence measurements were taken at

an excitation maximum wavelength of 460 nm and the emission maximum wavelength of 650 nm for acridine orange. The presence of the protein on the chip surface was confirmed by imaging the Sypro stain under a fluorescent microscope at a wavelength of 488 nm.

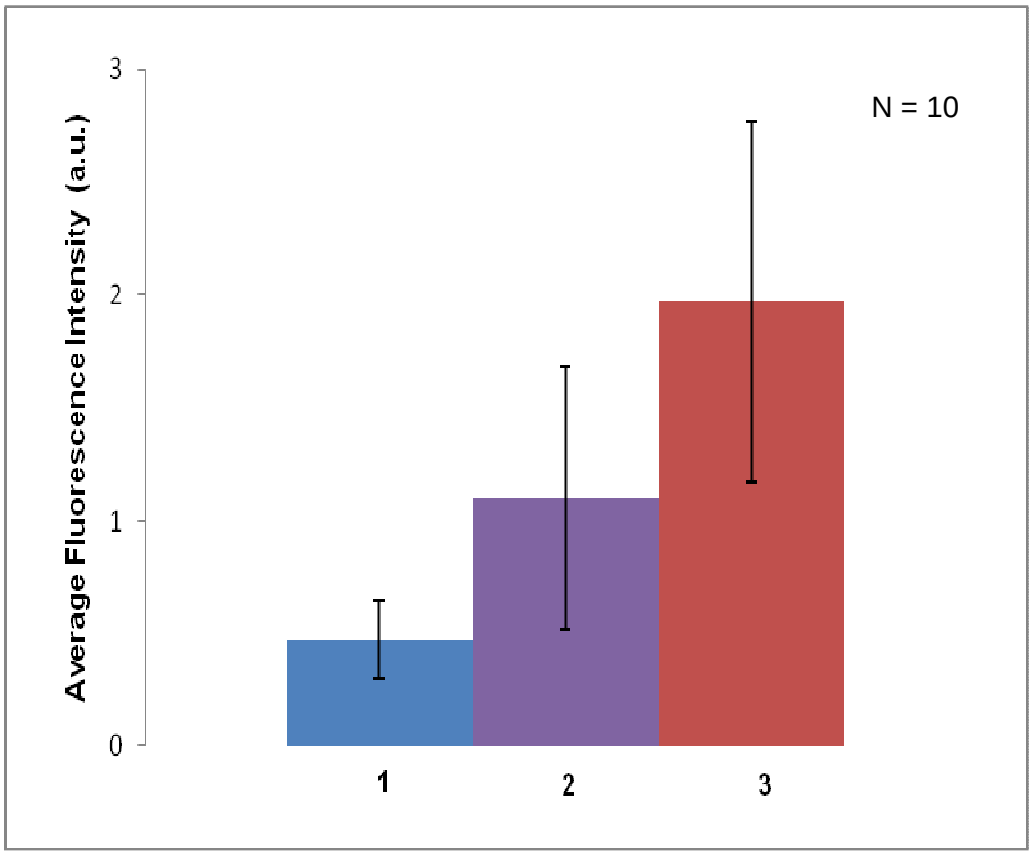

Figure 6.1 Acridine orange staining to confirm the presence of RNA aptamer on the titanium oxide chip surface. From L to R: Chip 1 – Control chip with APTES modification stained with acridine orange; Chip 2– Chip with mutant RNA aptamer immobilized; Chips 3 – Chip with RNA aptamer immobilized

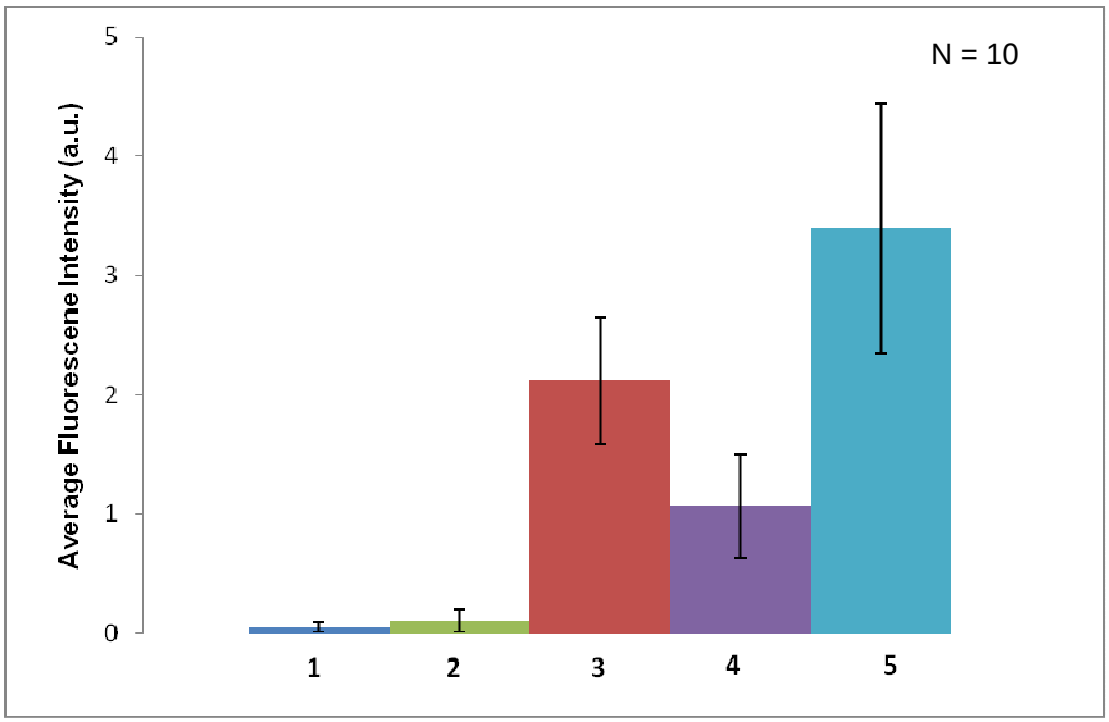

Figure 6.2 Sypro staining to confirm the presence of protein on the titanium oxide chip surface. From L to R: Chip 1 – Control chip with APTES modification; Chip 2 – Control chip with PDITC; Chip 3 – Control chip with PDITC and EGFR protein; Chip 4 - Control chip with mutant RNA and EGFR protein; Chip 5 – Chip with RNA aptamer and EGFR protein.

6.3.2 Resonance Shift Measurements

Initial resonance shift measurements were performed on a polyacrylate 96 well micro titer plate coated with titanium dioxide. The results obtained from the analysis showed the attachment of the RNA aptamer on the titanium dioxide and the EGFR protein capture by the RNA aptamer and not the mutant RNA.

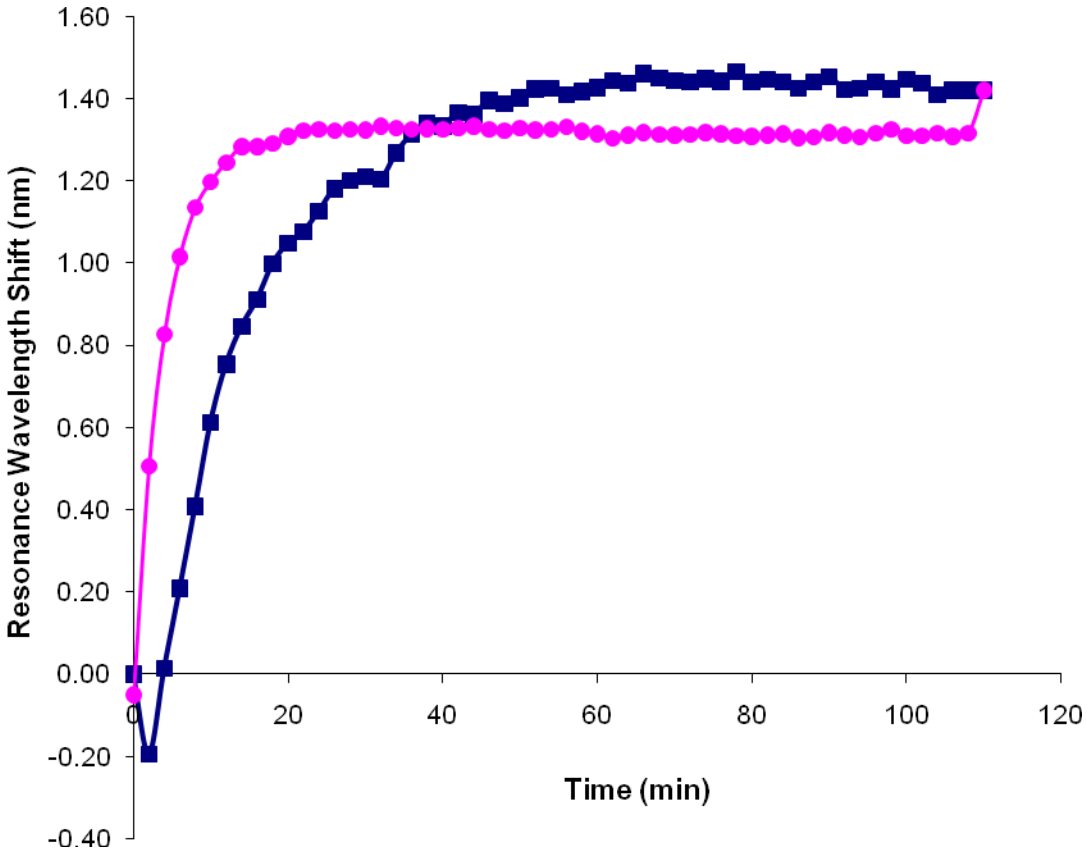

Figure 6.3 Resonance wavelength shift measurements showing the RNA aptamer (pink circle) and mutant RNA attachment (blue sqaure) attachment on the titanium oxide plate

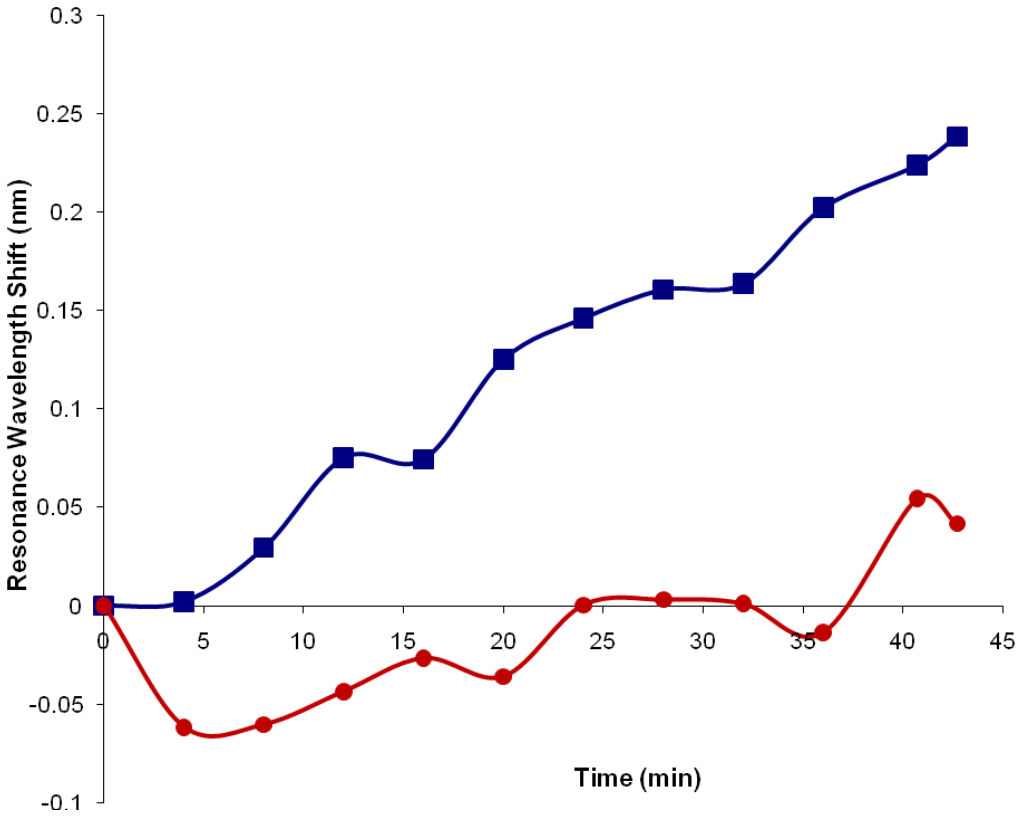

Figure 6.4 Resonance wavelength shift measurements showing the EGFR protein attachment with the RNA aptamer (blue square) and not the mutant RNA (red circles)

6.4 Discussion

The guided-mode resonance measurements show the attachment occurring between the titanium dioxide surface and the RNA aptamer. The data also show the protein capture by the RNA aptamer. The reasoning behind the obtained results is discussed in the following sections.

6.4.1 Surface Modification

The surface modifications were performed as mentioned in the earlier section. During the surface modification experiments, there were a few issues that needed to be addressed. Initially, the polyacrylate plates were diced into smaller chips and used for initial analysis using the respective stains. The

polyacrylate substrate, being a polymer, is sensitive to many solvents. So care had to be taken so as not to use the wrong solvent that would dissolve the substrate, The APTES solution used for silanization is made in ethanol. The polyacrylate substrate was found to degrade if immersed in ethanol for long periods of time. Hence, the reaction time was shortened and the concentration of the APTES was increased. This proved effective in getting a silane layer and not affecting the substrate. Usually, the PDITC is made in a DMF solution. When DMF was used with the polyacrylate, it completely dissolved when immersed in DMF for a little over 6 hours. Hence, the solvent was changed to DMSO.

During later experiments, instead of the diced chips, a 96 well micro titer plate coated with titanium dioxide with the same polyacrylate substrate was used. When using DMSO, during the experiment, it was observed that the well separator was being affected by the DMSO solvent. The separator degraded and left black colored residues on the titanium dioxide surface. In order to overcome these issues, a 2 inch silicon wafer was coated with titanium dioxide. And experiments were performed on it. The change of the substrate ensured that effective results were obtained.

6.4.2 Optical Detection of RNA Aptamer and Protein

The graph in figure 6.1 confirms the immobilization of RNA aptamer and the mutant RNA on titanium dioxide surface. As the RNA is a single stranded molecule, the fluorescence measurements were performed at an emission wavelength of 460 nm. The graph in Fig. 6.2 confirms the selective protein capture by RNA aptamer and not the mutant aptamer. In the graph it is seen that there is a high fluorescence intensity being recorded on the chip with the PDITC modification and protein flown on it. This can be explained by the fact that, proteins have many amine groups in them as an integral part of their structure. These amine groups are usually used up in the formation of peptide bonds. But in the cases of amino acids, such as lysine and arginine, that have amine side chains, the amine groups are available for reactions. These amine groups react with the diisothiocyanate groups in the PDITC and form bonds with them. This leads to the non-specific protein binding on PDITC modified chips. But it can be

seen that there is more protein binding seen on the chip with the aptamer rather than on the control chips. This shows the sensitivity and specificity of the aptamer for the EGFR protein.

While performing experiments with the polyacrylate substrate coated with titanium dioxide, after replacing the DMF solvent with DMSO, the substrates were seen to be stable and not degrade in the solvent. However, when trying to image the chips under a fluorescent microscope, a new problem arose, in that the thickness of the chips was an issue in adjusting the depth of focus. Hence, well focused images could not be obtained. In order to overcome the problem, a 2 inch silicon wafer was coated with titanium dioxide and the wafer was diced into smaller chips and used for experiments. This proved to be very fruitful as the attachment chemistry was performed on titanium dioxide chips and effective results were obtained from it.

In the aptamer immobilization experiments performed on the titanium dioxide surface, some of the initial experiments had to be repeated as the RNA aptamer was used without the DNA extension with the amine modification. The results obtained from those runs of experiments were deemed erroneous and not reported.

6.4.3 Resonance Shift Measurements

The resonance shift measurements were not performed in the clean room like the other experiments as the Vides Benchtop Plate Reader was located in a different lab and was integrated with a computer and could not be shifted to the clean room. The experiments were performed with the same amount of care and precision as when performed in the clean room. The results from the Figures 6.3 and 6.4 confirm the aptamer and protein attachment on the surface of the titanium oxide plate. The binding events were seen in real-time.

The results obtained from the wavelength shift measurements in the figures 6.5 and 6.6 also confirm the protein capture by the RNA aptamer. But as the wavelength shift values were close, the experiments were repeated in order to make sure there was no background interference in the results

obtained by the different buffers used in the attachments of the RNA aptamer and the protein. This was corrected in the repeated experiment and protein capture by the RNA aptamer was observed.

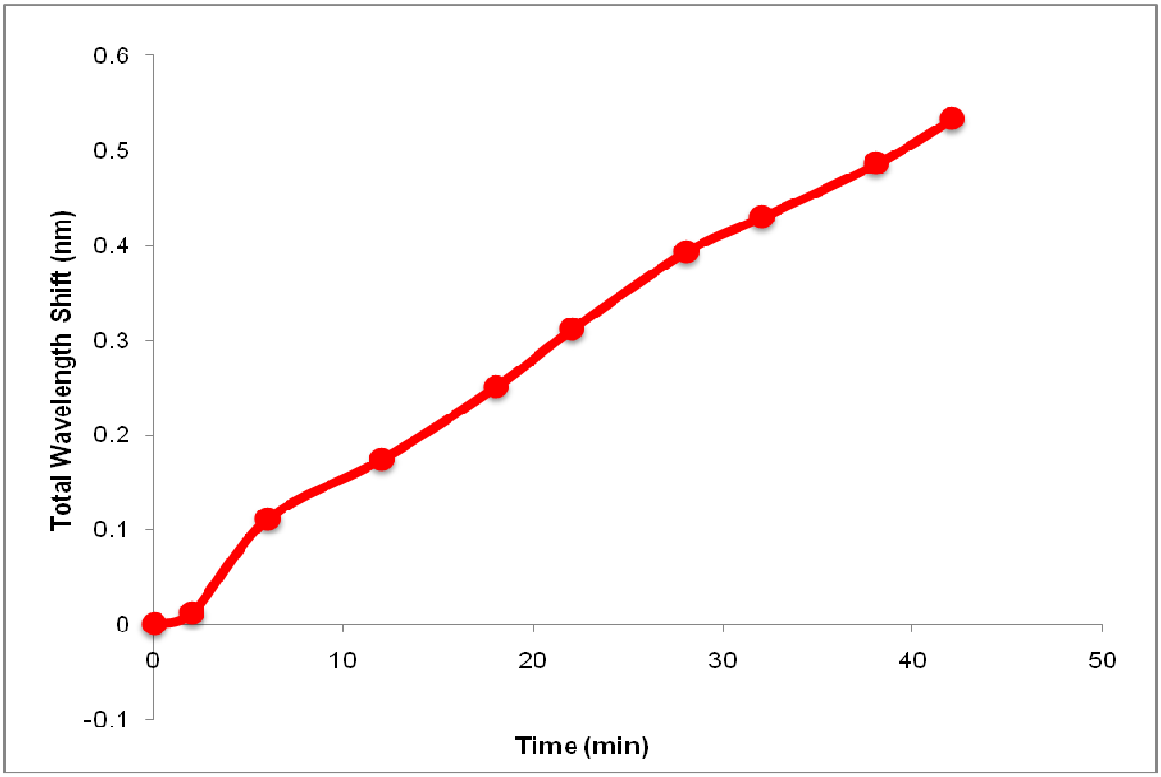

Figure 6.5 Wavelength shift measurement showing the real-time attachment of EGFR protein with the RNA aptamer

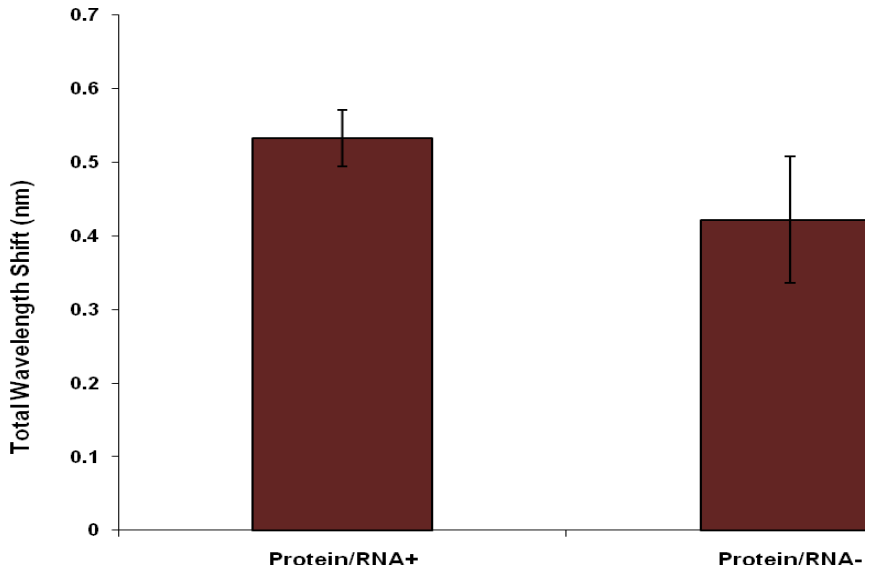

Figure 6.6 Wavelength shift measurements showing the protein capture by the RNA aptamer (Protein/RNA+) when compared with (Protein/RNA-)

6.5 Conclusion

From the experiments described it was seen that the protein capture by the EGFR RNA aptamer could be detected in real-time by the guided-mode resonance technology. A concentration of 50 ng/μL of protein was detected. The obtained results demonstrate that the aptamer and protein capture can be effectively coupled to any detection modality.

CHAPTER 7

SUMMARY AND OUTLOOK

The works discussed here completely fulfill the initial goal of designing a biochip for the detection of proteins. With the use of the R2Bm protein and dsDNA, the initial idea of electrical detection of dsDNA immobilization and protein detection was demonstrated. With the CMOS chip, a new detection limit was set at 2.8 fmol. This shows the sensitivity of the device and technology discussed. The use of Sypro Ruby Protein Blot stain on chip surfaces is also being discussed for the first time, as the stain is most commonly used only in gel electrophoreses experiments.

In order to demonstrate a practical application of the device in a biological setting, cancer protein, EGFR was detected. A CMOS chip with break junctions in the nano-scale range was fabricated. The fabrication of the break junctions using FIB showcases the novel method of introducing nano gaps in CMOS chips. An EGFR protein concentration of 50 ng/µL was detected using the CMOS chip.

The RNA aptamer was also immobilized on the titanium dioxide surface for detections based on guided-mode resonance. The wavelength shift measurements also confirmed the EGFR protein capture by the RNA aptamer. The capture of the EGFR protein with the anti-EGFR RNA aptamer has been reported for the very first time only in this thesis.

The usage of aptamers as the selective agent in the biochip is advantageous as the aptamers have higher selectivity for the target molecules than monoclonal antibodies. The non-antibody based detection reported in all the sections of the thesis are aimed towards bionanotechnology advancement in biochip and biosensor design. It can be said with confidence that refinement of the process will lead to higher sensitivities and better yield. The usage of different surfaces and different surface modifications

show the flexibilities possible in using aptamers as the selective agents. It also highlights how stable the aptamers are under various physical conditions.

The works reported here have most definitely paved the way for the design of more efficient biochips using aptamers as selective agents. The CMOS chips used in the experiments can be integrated on a larger area to form a microarray with each section of the array dedicated to the detection of an individual biomarker. With the detection of individual biomarkers, many disease conditions can be detected with the same sample source.

The application of the chips could also be extended to environmental sample analysis as well, such as in bioterrorism to identify dangerous virus or bacteria or to identify contaminants in food and water, etc. The versatility of the aptamers can be exploited for other applications as well, such as sample preparation which requires concentration of samples with a particular biomolecule.

REFERENCES

1. Dalton WS, Friend SH: **Cancer Biomarkers--An Invitation to the Table.** *Science* 2006, **312:**1165-1168.
2. Rifai N, Gillette MA, Carr SA: **Protein biomarker discovery and validation: the long and uncertain path to clinical utility.** *Nature biotechnology* 2006, **24:**971-984.
3. Golde TE, Eckman CB, Younkin SG: **Biochemical detection of A isoforms: implications for pathogenesis, diagnosis, and treatment of Alzheimer's disease.** *BBA-Molecular Basis of Disease* 2000, **1502:**172-187.
4. Hardy J: **Amyloid, the presenilins and Alzheimer's disease.** *Trends in neurosciences* 1997, **20:**154-159.
5. Selkoe DJ: **Alzheimer's disease: genes, proteins, and therapy.** *Physiological reviews* 2001, **81:**741.
6. Kurebayashi J: **Biomarkers in breast cancer.** *Cancer & chemotherapy* 2004, **31:**1021.
7. Klijn JG, Berns PM, Schmitz PI, Foekens JA: **The clinical significance of epidermal growth factor receptor (EGF-R) in human breast cancer: a review on 5232 patients.** *Endocrine reviews* 1992, **13:**3.
8. Yim EK, Park JS: **Role of proteomics in translational research in cervical cancer.** *Expert Review of Proteomics* 2006, **3:**21-36.
9. Kersemaekers AMF, Fleuren GJ, Kenter GG, Van den Broek L, Uljee SM, Hermans J, Van de Vijver MJ: **Oncogene alterations in carcinomas of the uterine cervix: overexpression of the epidermal growth factor receptor is associated with poor prognosis.** *Clinical Cancer Research* 1999, **5:**577.
10. Lopez JB: **Recent developments in the first detection of hepatocellular carcinoma.** *Clinical Biochemist Reviews* 2005, **26:**65.
11. Lynch TJ, Bell DW, Sordella R, Gurubhagavatula S, Okimoto RA, Brannigan BW, Harris PL, Haserlat SM, Supko JG, Haluska FG: **Activating mutations in the epidermal growth factor receptor underlying responsiveness of non-small-cell lung cancer to gefitinib.** *New England Journal of Medicine* 2004, **350:**2129-2139.
12. Hirsch FR, Varella-Garcia M, Bunn PA, Jr., Franklin WA, Dziadziuszko R, Thatcher N, Chang A, Parikh P, Pereira JR, Ciuleanu T, et al: **Molecular Predictors of Outcome With Gefitinib in a Phase III Placebo-Controlled Study in Advanced Non-Small-Cell Lung Cancer.** *J Clin Oncol* 2006, **24:**5034-5042.
13. Mellon K, Wright C, Kelly P, Horne CHW, Neal DE: **Original Articles: Bladder Cancer: Long-Term Outcome Related to Epidermal Growth Factor Receptor Status in Bladder Cancer.** *The Journal of urology* 1995, **153:**919-925.
14. Sheng KH, Yao YC, Chuang SS, Wu H, Wu TF: **Search for the tumor-related proteins of transition cell carcinoma in Taiwan by proteomic analysis.** *Proteomics* 2006, **6:**1058-1065.
15. Ahmed N, Oliva K, Barker G, Hoffmann P, Reeve S, Smith I, Quinn M, Rice G: **Proteomic tracking of serum protein isoforms as screening biomarkers of ovarian cancer.** *Proteomics* 2005, **5:**4625-4636.
16. Fischer-Colbrie J, Witt A, Heinzl H, Speiser P, Czerwenka K, Sevelda P, Zeillinger R: **EGFR and steroid receptors in ovarian carcinoma: comparison with prognostic parameters and outcome of patients.** *Anticancer research* 1997, **17:**613-619.

17. Ye B, Cramer DW, Skates SJ, Gygi SP, Pratomo V, Fu L, Horick NK, Licklider LJ, Schorge JO, Berkowitz RS: **Haptoglobin- Subunit As Potential Serum Biomarker in Ovarian Cancer.** *Clinical cancer research* 2003, **9:**2904.
18. Inada S, Koto T, Futami K, Arima S, Iwashita A: **Evaluation of malignancy and the prognosis of esophageal cancer based on an immunohistochemical study (p53, E-cadherin, epidermal growth factor receptor).** *Surgery Today* 1999, **29:**493-503.
19. Nishimori T, Tomonaga T, Matsushita K, Oh-Ishi M, Kodera Y, Maeda T, Nomura F, Matsubara H, Shimada H, Ochiai T: **Proteomic analysis of primary esophageal squamous cell carcinoma reveals downregulation of a cell adhesion protein, periplakin.** *Proteomics* 2006, **6:**1011-1018.
20. Strehlitz B, Nikolaus N, Stoltenburg R: **Protein detection with aptamer biosensors.** *Sensors* 2008, **8:**4296-4307.
21. Cooper MA: **Optical biosensors in drug discovery.** *Nature Reviews Drug Discovery* 2002, **1:**515-528.
22. Xu D, Xu D, Yu X, Liu Z, He W, Ma Z: **Label-free electrochemical detection for aptamer-based array electrodes.** *Analytical chemistry(Washington, DC)* 2005, **77:**5107-5113.
23. Rodriguez MC, Kawde AN, Wang J: **Aptamer biosensor for label-free impedance spectroscopy detection of proteins based on recognition-induced switching of the surface charge.** *Chemical Communications* 2005, **2005:**4267-4269.
24. Niemeyer CM: **Nanoparticles, proteins, and nucleic acids: biotechnology meets materials science.** *Angew Chem Int Ed* 2001, **40:**4128-4158.
25. Cui Y, Wei Q, Park H, Lieber CM: **Nanowire nanosensors for highly sensitive and selective detection of biological and chemical species.** *Science* 2001, **293:**1289.
26. Zheng G, Patolsky F, Cui Y, Wang WU, Lieber CM: **Multiplexed electrical detection of cancer markers with nanowire sensor arrays.** *Nature Biotechnology* 2005, **23:**1294-1301.
27. Jensenius H, Thaysen J, Rasmussen AA, Veje LH, Hansen O, Boisen A: **A microcantilever-based alcohol vapor sensor-application and response model.** *Applied Physics Letters* 2000, **76:**2615.
28. Chen RJ, Choi HC, Bangsaruntip S, Yenilmez E, Tang X, Wang Q, Chang YL, Dai H: **An investigation of the mechanisms of electronic sensing of protein adsorption on carbon nanotube devices.** *Nano Lett* 2003, **3:**727.
29. Yu X, Munge B, Patel V, Jensen G, Bhirde A, Gong JD, Kim SN, Gillespie J, Gutkind JS, Papadimitrakopoulos F: **Carbon nanotube amplification strategies for highly sensitive immunodetection of cancer biomarkers.** *Journal of the American Chemical Society* 2006, **128:**11199.
30. Star A, Gabriel JCP, Bradley K, Gruner G: **Electronic detection of specific protein binding using nanotube FET devices.** *Nano Letters* 2003, **3:**459-463.
31. Indyk HE, Filonzis EL: **Direct optical biosensor analysis of folate-binding protein in milk.** *J Agric Food Chem* 2004, **52:**3253-3258.
32. Henne WA, Doorneweerd DD, Lee J, Low PS, Savran C: **Detection of folate binding protein with enhanced sensitivity using a functionalized quartz crystal microbalance sensor.** *Anal Chem* 2006, **78:**4880-4884.
33. Bao YP, Wei TF, Lefebvre PA, An H, He L, Kunkel GT, Muller UR: **Detection of protein analytes via nanoparticle-based bio bar code technology.** *Anal Chem* 2006, **78:**2055-2059.
34. Loo RW, Tam PL, Goh JB, Goh MC: **An enzyme-amplified diffraction-based immunoassay.** *Analytical biochemistry* 2005, **337:**338-342.
35. Hongquan Zhang ZWX-FLXCL: **Ultrasensitive Detection of Proteins by Amplification of Affinity Aptamers.** *Angewandte Chemie* 2006, **118:**1606-1610.
36. Chou SH, Chin KH, Wang AHJ: **DNA aptamers as potential anti-HIV agents.** *Trends in Biochemical Sciences* 2005, **30:**231-234.
37. Hamaguchi N, Ellington A, Stanton M: **Aptamer Beacons for the Direct Detection of Proteins.** *Analytical Biochemistry* 2001, **294:**126-131.

38. Maehashi K, Katsura T, Kerman K, Takamura Y, Matsumoto K, Tamiya E: **Label-Free Protein Biosensor Based on Aptamer-Modified Carbon Nanotube Field-Effect Transistors.** *Anal Chem* 2007, **79:**782-787.
39. Ylera F, Lurz R, Erdmann VA, Furste JP: **Selection of RNA Aptamers to the Alzheimer's Disease Amyloid Peptide.** *Biochemical and Biophysical Research Communications* 2002, **290:**1583-1588.
40. Fischer NO, Tarasow TM, Tok JBH: **Aptasensors for biosecurity applications.** *Current Opinion in Chemical Biology* 2007, **11:**316-328.
41. De Soultrait VR, Lozach PY, Altmeyer R, Tarrago-Litvak L, Litvak S, Andreola ML: **DNA aptamers derived from HIV-1 RNase H inhibitors are strong anti-integrase agents.** *Journal of molecular biology* 2002, **324:**195-203.
42. Feigon J, Dieckmann T, Smith FW: **Aptamer structures from A to z.** *Chemistry and Biology-London* 1996, **3:**611-618.
43. Conrad R, Ellington AD: **Detecting immobilized protein kinase C isozymes with RNA aptamers.** *Analytical biochemistry* 1996, **242:**261-265.
44. Proske D, Hofliger M, Soll RM, Beck-Sickinger AG, Famulok M: **A Y2 receptor mimetic aptamer directed against neuropeptide Y.** *Journal of Biological Chemistry* 2002, **277:**11416-11422.
45. Brody EN, Willis MC, Smith JD, Jayasena S, Zichi D, Gold L: **The use of aptamers in large arrays for molecular diagnostics.** *Molecular Diagnosis* 1999, **4:**381-388.
46. Burgstaller P, Girod A, Blind M: **Aptamers as tools for target prioritization and lead identification.** *Drug discovery today* 2002, **7:**1221-1228.
47. Green LS, Bell C, Janjic N: **Aptamers as reagents for high-throughput screening.** *Biotechniques* 2001, **30:**1094.
48. Bang GS, Cho S, Kim BG: **A novel electrochemical detection method for aptamer biosensors.** *Biosensors and Bioelectronics* 2005, **21:**863-870.
49. Klug SJ, Famulok M: **All you wanted to know about SELEX.** *Molecular biology reports* 1994, **20:**97-107.
50. Eulberg D, Buchner K, Maasch C, Klussmann S: **Development of an automated in vitro selection protocol to obtain RNA-based aptamers: identification of a biostable substance P antagonist.** *Nucleic Acids Research* 2005, **33:**e45.
51. Cox JC, Ellington AD: **Automated selection of anti-protein aptamers.** *Bioorganic & medicinal chemistry* 2001, **9:**2525-2531.
52. Proske D, Blank M, Buhmann R, Resch A: **Aptamers—basic research, drug development, and clinical applications.** *Applied microbiology and biotechnology* 2005, **69:**367-374.
53. Love JC, Estroff LA, Kriebel JK, Nuzzo RG, Whitesides GM: **Self-assembled monolayers of thiolates on metals as a form of nanotechnology.** *Chem Rev* 2005, **105:**1103-1170.
54. Lobert PE, Bourgeois D, Pampin R, Akheyar A, Hagelsieb LM, Flandre D, Remacle J: **Immobilization of DNA on CMOS compatible materials.** *Sensors & Actuators: B Chemical* 2003, **92:**90-97.
55. Carpenter G CS: **Epidermal growth factor.** *J Biol Chem* 1990, **265:**7709-7712
56. Rude Voldborg B, Damstrup L, Spang-Thomsen M, Skovgaard Poulsen H: **Epidermal growth factor receptor (EGFR) and EGFR mutations, function and possible role in clinical trials.** *Annals of Oncology* 1997, **8:**1197-1206.
57. Christensen SM, Bibillo A, Eickbush TH: **Role of the Bombyx mori R2 element N-terminal domain in the target-primed reverse transcription (TPRT) reaction.** *Nucleic acids research* 2005, **33:**6461.
58. Malik HS, Burke WD, Eickbush TH: **The age and evolution of non-LTR retrotransposable elements.** *Molecular biology and evolution* 1999, **16:**793.
59. Kojima KK, Fujiwara H: **Cross-genome screening of novel sequence-specific non-LTR retrotransposons: various multicopy RNA genes and microsatellites are selected as targets.** *Molecular biology and evolution* 2004, **21:**207.

60. Burke WD, Malik,H.S., Jones,J.P. and Eickbush,T.H.: **The domain structure and retrotransposition mechanism of R2 elements 75 are conserved throughout arthropods.** *Mol Biol Evol* 1999, **16:**506 - 511.
61. Christensen SM, Eickbush TH: **R2 target-primed reverse transcription: ordered cleavage and polymerization steps by protein subunits asymmetrically bound to the target DNA.** *Molecular and Cellular Biology* 2005, **25:**6617-6628.
62. Blanco FJ, Agirregabiria M, Garcia J, Berganzo J, Tijero M, Arroyo MT, Ruano JM, Aramburu I, Mayora K: **Novel three-dimensional embedded SU-8 microchannels fabricated using a low temperature full wafer adhesive bonding.** *Journal of Micromechanics and Microengineering* 2004, **14:**1047-1056.
63. P.P. Ramachandran S. M. Christensen, S.M. Iqbal: **Electronic Detection of Selective Proteins using Non Antibody-Based CMOS Chip.** In *IEEE/NIH Life Science Systems and Applications Workshop (LiSSA 2009); Bethesda, Maryland*. 2009
64. Moreland J, Ekin JW: **Electron tunneling experiments using Nb Sn ''break''junctions.** *Journal of Applied Physics* 1985, **58:**3888.
65. Tibuleac S, Wawro D, Magnusson R: **'Resonant diffractive structures integrating waveguide gratings on optical fiber endfaces.** In.;
66. Magnusson R, Wang SS: **New principle for optical filters.** *Applied Physics Letters* 1992, **61:**1022.
67. Wawro DD, Tibuleac S, Magnusson R, Liu H: **Optical fiber endface biosensor based on resonances in dielectric waveguide gratings.** In.; 2000: 86.
68. Manning M, Harvey S, Galvin P, Redmond G: **A versatile multi-platform biochip surface attachment chemistry.** *Materials Science & Engineering C* 2003, **23:**347-351.
69. http://rsbweb.nih.gov/ij/.
70. McMaster GK, Carmichael GG: **Analysis of single-and double-stranded nucleic acids on polyacrylamide and agarose gels by using glyoxal and acridine orange.** *Proceedings of the National Academy of Sciences* 1977, **74:**4835.
71. Traganos F, Darzynkiewicz Z, Sharpless T, Melamed MR: **Simultaneous staining of ribonucleic and deoxyribonucleic acids in unfixed cells using acridine orange in a flow cytofluorometric system.** *Journal of Histochemistry and Cytochemistry* 1977, **25:**46.
72. Lopez MF, Berggren K, Chernokalskaya E, Lazarev A, Robinson M, Patton WF: **A comparison of silver stain and SYPRO Ruby Protein Gel Stain with respect to protein detection in two-dimensional gels and identification by peptide mass profiling.** *ELECTROPHORESIS* 2000, **21:**3673-3683.

BIOGRAPHICAL INFORMATION

Priyanka Pachampettai Ramachandran was born in Chennai, India, in November 1985. She finished her schooling in her hometown and did her undergraduate studies from The Anna University, Chennai, India in Industrial Biotechnology. She is interested in pursuing a career in cancer research deciphering the different biomarkers that could lead to early diagnosis. Towards this goal she joined the Nano Bio Lab in January 2008. Here, she has indentified biomarker proteins and helped design a device for the protein detection.